Published for SISSA by Springer

Received: *September 17, 2024*
Accepted: *November 28, 2024*
Published: *December 27, 2024*

Improved π^0, η, η' transition form factors in resonance chiral theory and their a_μ^{HLbL} contribution

Emilio J. Estrada,[a] **Sergi Gonzàlez-Solís**,[b,c] **Adolfo Guevara**[d] **and Pablo Roig**[a,e]

[a] *Departamento de Física, Centro de Investigación y de Estudios Avanzados del Instituto Politécnico Nacional,*
Apdo. Postal 14-740, 07000 Ciudad de México, México
[b] *Departament de Física Quàntica i Astrofísica, Universitat de Barcelona,*
Martí i Franquès, 1, 08028 Barcelona, Spain
[c] *Institut de Ciències del Cosmos, Universitat de Barcelona,*
Martí i Franquès, 1, 08028 Barcelona, Spain
[d] *Área Académica de Matemáticas y Física, Universidad Autónoma del Estado de Hidalgo,*
Carretera Pachuca-Tulancingo Km. 4.5, C.P. 42184, Pachuca, Hgo., México
[e] *IFIC, Universitat de València – CSIC,*
Catedrático José Beltrán 2, E-46980 Paterna, Spain

E-mail: emilio.estrada@cinvestav.mx, sergig@icc.ub.edu, adolfo_guevara@uaeh.edu.mx, pablo.roig@cinvestav.mx

Abstract: Working with Resonance Chiral Theory, within the two resonance multiplets saturation scheme, we satisfy leading (and some subleading) chiral and asymptotic QCD constraints and accurately fit simultaneously the π^0, η, η' transition form factors, for single and double virtuality. In the latter case, we supplement the few available measurements with lattice data to ensure a faithful description. Mainly due to the new results for the doubly virtual case, we improve over existing descriptions for the η and η'. Our evaluation of the corresponding pole contributions to the hadronic light-by-light piece of the muon $g-2$ read: $a_\mu^{\pi^0\text{-pole}} = \left(61.9 \pm 0.6^{+2.4}_{-1.5}\right) \times 10^{-11}$, $a_\mu^{\eta\text{-pole}} = \left(15.2 \pm 0.5^{+1.1}_{-0.8}\right) \times 10^{-11}$ and $a_\mu^{\eta'\text{-pole}} = \left(14.2 \pm 0.7^{+1.4}_{-0.9}\right) \times 10^{-11}$, for a total of $a_\mu^{\pi^0+\eta+\eta'\text{-pole}} = \left(91.3 \pm 1.0^{+3.0}_{-1.9}\right) \times 10^{-11}$, where the first and second errors are the statistical and systematic uncertainties, respectively.

Keywords: Chiral Lagrangian, Effective Field Theories of QCD

ArXiv ePrint: 2409.10503

https://doi.org/10.1007/JHEP12(2024)203

Contents

1 Introduction

The anomalous magnetic moment of the muon ($a_\mu = (g_\mu - 2)/2$, with g the gyromagnetic factor) has been one of the most attractive observables in recent years, given its extremely precise measurements [1–3] and Standard Model predictions [4][1] and the persistent discrepancy between them, which seems to be reducing lately [82, 87, 91, 96, 97]. While the experimental uncertainty on a_μ has shrunk up to 22×10^{-11}, and will likely be $\lesssim 16 \times 10^{-11}$ after the final FNAL measurement, the error of the theory prediction is not at the same level at the moment.

This uncertainty is dominated by the hadronic interaction contributions in the non-perturbative regime of QCD, where hadrons play the key rôle. Among these, the hadronic vacuum polarization (HVP) part dominates the error, yielding 40 of the 43 units (in 10^{-11}) of the overall uncertainty, the rest coming from the sum in quadrature of this error with the one stemming from the hadronic light-by-light (HLbL) piece, 17×10^{-11}. The uncertainty of the HVP part in the new evaluation of ref. [91] (33×10^{-11}) is, however, smaller than the one in the White Paper [4]. The error in ref. [91] still basically doubles that of the HLbL contribution, which is commensurate with the expected uncertainty of the final FNAL a_μ publication. Therefore, although not pressing now, the need to improve over existing computations of $a_\mu^{\rm HLbL}$ will be intensified by the time the $a_\mu^{\rm HVP}$ picture becomes clearer (the most recent developments seem to be pointing that way). In this context, it is the purpose of this work to advance in the understanding of the dominant contribution to $a_\mu^{\rm HLbL}$ (yielding

[1]The Standard Model prediction in the White Paper [4] is based on refs. [5–39]. This field has been evolving very actively since ref. [4] was published. See e.g., refs. [40–95].

JHEP12(2024)203

its whole value [4] at 68% C.L.[2] $\sim 93 \times 10^{-11}$), given by the lightest pseudoscalar poles: those corresponding to the π^0, η and η' mesons, $a_\mu^{P\text{-poles, HLbL}}$.

It was soon realized that the bulk of a_μ^{HLbL} comes from the P-poles contribution [98–104]. Noticeably, the usefulness of the limit of QCD for a large number of colors (N_C) [105–107] and the chiral counting [108–110] were acknowledged in comprehending the relative size of the various contributions to a_μ^{HLbL} and their numerical ballpark values [98, 100, 101, 104]. Large-N_C QCD and the short-distance constraints of the strong interactions were the guiding principles in ref. [111], which was a key source for later evaluations of $a_\mu^{P\text{-poles, HLbL}}$. Particularly, the short-distance behaviour of the form-factor entering the real photon vertex was challenged in ref. [21] and the importance of axial-vector mesons contributions in fulfilling asymptotic QCD was put forward, a topic which has advanced notably since then (see e.g. refs. [30, 33, 42–45, 49, 51, 54, 55, 58, 72, 73, 79, 112–118]).

We recapitulate the situation for $a_\mu^{P\text{-poles, HLbL}}$ by the White Paper. The π^0 contribution was taken from the dispersive evaluation [24], which agreed with an earlier computation based on rational approximants [22]. The latter was the one taken for the $\eta^{(\prime)}$ contributions, for which a numerical dispersive result has not been published yet. Dyson-Schwinger evaluations [119, 120] and the lattice QCD computation [25] (including only the π^0) agreed with them within errors. These results are summarized in the first rows of table 10, yielding the data-driven prediction $a_\mu^{P\text{-poles, HLbL}} = \left(93.8^{+4.0}_{-3.6}\right) \times 10^{-11}$ [4]. The numerical values of other data-driven calculations of $a_\mu^{P\text{-poles, HLbL}}$ were not quoted in the White Paper [4], because they failed to satisfy the quality criteria listed just before its section 4.4.1., which we copy here — for reference — at the beginning of section 5.

This was precisely the case of computations using Resonance Chiral Lagrangians [121]: refs. [122, 123] and [124], which added flavor-symmetry breaking corrections to the previous two calculations (see also ref. [125]). In particular, including just one multiplet of vector mesons it was not possible to comply with the leading asymptotic behaviour for double virtuality, thus violating the last part of the first requirement for the White Paper [4]. In ref. [124], the associated error was estimated to be $\left(^{+5.0}_{-0.0}\right) \times 10^{-11}$, from the contribution of excited vector multiplets, which would restore the appropriate short-distance behaviour for double virtuality. In this work we have verified previous results and computed all new contributions associated to the first resonance excitations within this formalism, being consistent with the procedure of ref. [124] and complying now with the QCD short-distance behaviour.[3]

Resonance Chiral Theory (RχT) [121] is an effective approach that adds, to the Chiral Perturbation Theory (χPT) action [108, 109], the light-flavored resonances as active fields. This is done without any assumption on the resonance dynamics. In this way, one can for instance see the celebrated notion of vector meson dominance emerging as a result of integrating out the resonance fields and checking that the next-to-leading order chiral low-energy constants are essentially saturated by the corresponding contributions to the chiral

[2] It must be clarified that it contributes to the a_μ^{HLbL} uncertainty, 17×10^{-11}, only with 5×10^{-11} directly, although its dominant part may be ascribed to the interplay of P and axial poles, related to the fulfillment of QCD short-distance constraints and the chiral anomaly, as commented in the next paragraph.

[3] A more complicated solution, including three resonance multiplets, was worked out in ref. [126]. In this case it is possible to match even more subleading QCD asymptotic constraints. See table 11 for the comparison of our procedure to this reference.

JHEP12(2024)203

effective Lagrangian. We work within the large-N_C limit and assume a $1/N_C$ expansion (the small impact of subleading terms is considered in section 7.1). Thus, the spontaneous symmetry breaking pattern is $\mathrm{U}(3)_L \times \mathrm{U}(3)_R \to \mathrm{U}(3)_{L+R\sim V}$, so that the P pseudoscalars will be part of a nonet of pseudo-Goldstone bosons. We will consider the RχT Lagrangian pieces derived in refs. [121, 122, 127–132]. The restrictions imposed by perturbative QCD on the asymptotic behaviour of the P transition form factors will determine all but 12 parameters (including four describing the η-η' mixing), that will be fitted to the available spacelike data: the di-photon P decay widths, and the singly and doubly virtual measurements. For double virtuality, supplementing the very few points (only for the η') with lattice data will turn out to be fundamental.

As the main outcome of our work, we predict the following $a_\mu^{P\text{-poles, HLbL}}$ contributions (in units of 10^{-11}): $a_\mu^{\pi^0\text{-pole}} = \left(61.9 \pm 0.6^{+2.4}_{-1.5}\right)$, $a_\mu^{\eta\text{-pole}} = \left(15.2 \pm 0.5^{+1.1}_{-0.8}\right)$ and $a_\mu^{\eta'\text{-pole}} = \left(14.2 \pm 0.7^{+1.4}_{-0.9}\right)$, for a total of $a_\mu^{\pi^0+\eta+\eta'\text{-pole}} = \left(91.3 \pm 1.0^{+3.0}_{-1.9}\right)$, where the first uncertainty is statistical and the second one is the systematic theory error (discussed in detail in section 7.1).

The paper is organized as follows. In section 2, we review the relevant pieces of the resonance chiral Lagrangian. After that, in section 3, we introduce briefly the P transition form factors and focus on the new contributions, from the excited resonances, that were disregarded in ref. [124]. We start section 4 recalling the restrictions imposed by perturbative QCD on the asymptotic behaviour of the P transition form factors. Then, we apply them to our results, first in the chiral limit and then including $\mathcal{O}(m_P^2)$ corrections. The relations that we found on the resonance Lagrangian couplings are consistent with the restrictions obtained studying the VVP Green's function. Using these relations allows us to get more compact form factors, depending on 12 parameters, that are confronted to spacelike data (for real photons, and for the singly- and doubly-virtual cases) in section 5. We quote and discuss our best fit results, verifying their accuracy and consistency. Section 6 examines their correspondence with those obtained with Canterbury Approximants, explaining our preference for RχT. We compute the P-pole contributions to a_μ in section 7 and state our conclusions in section 8.

2 Resonance chiral theory Lagrangian

In this section we describe the formalism used to compute the P transition form factors, namely RχT,[4] which extends the energy domain of applicability of the χPT Lagrangian [109] by including the light-flavored resonances as explicit degrees of freedom [121].

The leading contribution to the $P\gamma\gamma$ transition form factor (TFF) at low energies[5] is given by the Wess-Zumino-Witten (WZW) contact term [133, 134], which is completely specified by the chiral anomaly [135, 136], in terms of the number of colours of the QCD gauge group (N_C) and the pion decay constant in the chiral limit (F). We will not quote here the WZW action (it can be found in e.g. appendix A of ref. [124]), but rather recall in the next section its contribution to the π^0, η and η' TFF. This one, being a constant, demands additional pieces to yield a behaviour complying with QCD constraints. Within RχT we will accomplish this by considering interactions mediated by vector mesons that will modify the

[4] A more extended discussion can be found in e.g. ref. [124].

[5] It is $\mathcal{O}(p^4)$ in the chiral expansion, where $p^2 \sim m_P^2$ [109].

JHEP12(2024)203

WZW local interaction. We will need to account for odd-intrinsic parity operators with a pseudo-Goldsonte boson and either two vector resonances, or one such resonance and a vector current. We will also need to include the non-resonant $R\chi T$ odd-intrinsic parity Lagrangian at $\mathcal{O}(p^6)$, which has the same operator structure as the χPT Lagrangian of the same order [137].

The complete basis of odd-intrinsic parity RχT operators which -upon resonance integration- saturate most of the $\mathcal{O}(p^6)$ chiral low-energy constants (LECs) was found in ref. [122]. We will, however, use the basis in ref. [127], which is sufficient for processes including just one pseudoscalar meson [138] and simpler (smaller) for the present study. To achieve a consistent description [122], we need to consider pseudoscalar resonances as well [124], which naturally come along with the second vector multiplet [123] that we introduce here in the context of the P TFF within RχT.

We organize the Lagrangian describing the lightest pseudo-Goldstone bosons and their interactions in increasing number of resonance fields, R:

$$\mathcal{L}_{\mathrm{R}\chi\mathrm{T}} = \mathcal{L}_{\text{no } R} + \sum_R (\mathcal{L}_R^{\mathrm{Kin}} + \mathcal{L}_{R'}^{\mathrm{Kin}}) + \sum_{R,R'} \mathcal{L}_{R,R'} + \cdots . \tag{2.1}$$

We will further divide the RχT Lagrangian into its odd- and even-intrinsic parity sectors, including, in addition to the pseudo-Goldstone bosons (φ^a) and the photons (γ), the two lightest vector meson multiplets ($V^{(\prime)}$) and the first pseudoscalar excitations (P').

Operators with no resonance fields.

This part of the Lagrangian will be formally equivalent to the χPT one. We must note, however, that the values of the chiral LECs vary from χPT to this sector of RχT precisely by the fact that in the latter the resonance degrees of freedom are active, whereas they have been integrated out in the former. The relevant part of $\mathcal{L}_{\text{no } R}$ in both intrinsic parity sectors reads ($\langle \ldots \rangle$ stands for a trace in flavor space):[6]

$$\mathcal{L}_{\text{no } R}^{\text{even}} = \frac{F^2}{4} \langle u_\mu u^\mu + \chi_+ \rangle , \quad \mathcal{L}_{\text{no } R}^{\text{odd}} = \mathcal{L}_{\mathrm{WZW}} + \sum_{j=7,8,22} C_j^W \mathcal{O}_j^W , \tag{2.2}$$

where we used the chiral tensors [139]

$$u_\mu = i \left[u^\dagger (\partial_\mu - i r_\mu) u - u (\partial_\mu - i l_\mu) u^\dagger \right] , \quad \chi_\pm = u^\dagger \chi u^\dagger \pm u \chi^\dagger u , \tag{2.3}$$

in which the external (pseudo)scalar $(p)s$ spin-zero and (left)-right $(l_\mu)r_\mu$ spin-one sources appear. For the vector electromagnetic case

$$r_\mu = l_\mu = eQA_\mu + \cdots , \quad Q = \mathrm{diag}\left(\frac{2}{3}, -\frac{1}{3}, -\frac{1}{3}\right) . \tag{2.4}$$

Explicit chiral symmetry breaking is introduced like in QCD, through non-vanishing quark masses, by means of the scalar current, via

$$\chi = 2B(s + ip), \quad s = \mathrm{diag}(m_u, m_d, m_s), \quad p = 0, \quad 2m = m_u + m_d, \tag{2.5}$$

[6] We include the $\mathcal{O}_j^W$ operators, which are subleading in the chiral expansion with respect to the WZW piece, to ensure the most general breaking of flavor symmetry. Nevertheless, our analysis of short-distance constraints will show that their coefficients, C_j^W, vanish.

JHEP12(2024)203

where the last equality corresponds to the isospin symmetry limit,[7] which is an excellent approximation in our study. In eq. (2.3), the operator u also appears, depending non-linearly on the pseudo-Goldstone bosons φ^a ($\sqrt{2}\Phi = \sum_{a=0}^{8} \varphi^a \lambda_a$, the η' becomes the ninth such boson in the chiral and large-N_C limits [105–107])

$$u = \exp\left(i\frac{\Phi}{\sqrt{2}F}\right), \tag{2.6}$$

through

$$\Phi = \begin{pmatrix} \frac{1}{\sqrt{2}}(C_\pi\pi^0 + C_q\eta + C'_q\eta') & \pi^+ & K^+ \\ \pi^- & \frac{1}{\sqrt{2}}(-C_\pi\pi^0 + C_q\eta + C'_q\eta') & K^0 \\ K^- & \bar{K}^0 & -C_s\eta + C'_s\eta' \end{pmatrix}. \tag{2.7}$$

In eq. (2.7), $C_\pi = F/F_\pi$ in the large-N_C limit [140–142], with the physical pion decay constant $F_\pi = 92.2\,\text{MeV}$ [143]. $C^{(\prime)}_{q,s}$ describe the η-η' system in the two-angle mixing scheme

$$C_q = \frac{F}{\sqrt{3}\cos(\theta_8 - \theta_0)}\left(\frac{\cos\theta_0}{f_8} - \frac{\sqrt{2}\sin\theta_8}{f_0}\right), \tag{2.8a}$$

$$C'_q = \frac{F}{\sqrt{3}\cos(\theta_8 - \theta_0)}\left(\frac{\sqrt{2}\cos\theta_8}{f_0} + \frac{\sin\theta_0}{f_8}\right), \tag{2.8b}$$

$$C_s = \frac{F}{\sqrt{3}\cos(\theta_8 - \theta_0)}\left(\frac{\sqrt{2}\cos\theta_0}{f_8} + \frac{\sin\theta_8}{f_0}\right), \tag{2.8c}$$

$$C'_s = \frac{F}{\sqrt{3}\cos(\theta_8 - \theta_0)}\left(\frac{\cos\theta_8}{f_0} - \frac{\sqrt{2}\sin\theta_0}{f_8}\right), \tag{2.8d}$$

in terms of two angles ($\theta_{8,0}$) and two couplings ($f_{8,0}$) [144–147].

The relevant operators entering $\mathcal{L}_{\text{no }R}$ in eq. (2.2) are ($\epsilon_{\mu\nu\rho\sigma}$ is common to all of them and omitted below, we use the standard convention $\epsilon_{0123} = +1$)[8]

$$\mathcal{O}_7^W = i\langle\chi_- f_+^{\mu\nu} f_+^{\rho\sigma}\rangle, \quad \mathcal{O}_8^W = i\langle\chi_-\rangle\langle f_+^{\mu\nu} f_+^{\rho\sigma}\rangle, \quad \mathcal{O}_{22}^W = \langle u^\mu \left\{\nabla_\lambda f_+^{\lambda\nu}, f_+^{\rho\sigma}\right\}\rangle, \tag{2.9}$$

where $f_\pm^{\mu\nu} = uF_L^{\mu\nu}u^\dagger \pm u^\dagger F_R^{\mu\nu}u$, and $F^{\mu\nu}_{L(R)} = \partial^\mu\ell(r)^\nu - \partial^\nu\ell(r)^\mu - i[\ell(r)^\mu, \ell(r)^\nu] = eQF^{\mu\nu} + \cdots$, in terms of the electromagnetic field-strength tensor, $F^{\mu\nu}$. The covariant derivative is defined as $\nabla_\mu \cdot = \partial_\mu \cdot + [\Gamma_\mu, \cdot]$, with the connection $\Gamma_\mu = \frac{1}{2}\left[u^\dagger(\partial_\mu - ir_\mu)u + u(\partial_\mu - il_\mu)u^\dagger\right]$. In eq. (2.9), only $\mathcal{O}_{22}$ does not induce U(3) symmetry breaking corrections.

Vector resonances and their kinetic terms.

We describe the resonances with antisymmetric tensor fields [121]. In the vector case, this corresponds to

$$V_{\mu\nu} = \begin{pmatrix} (\rho^0 + \omega^0)/\sqrt{2} & \rho^+ & K^{*+} \\ \rho^- & (-\rho^0 + \omega^0)/\sqrt{2} & K^{*0} \\ K^{*-} & \bar{K}^{*0} & \phi \end{pmatrix}_{\mu\nu}, \tag{2.10}$$

[7] The isospin symmetry limit corresponds to $m_u = m_d$, denoted here m, resulting in $m_u + m_d = 2m$.

[8] The operator $\mathcal{O}_8^W$ is suppressed in the $1/N_C$ expansion since it has a double-trace. We keep it because this type of corrections could in principle play a non-negligible rôle for the η-η' mesons [124].

JHEP12(2024)203

j	$\mathcal{O}^j_{VJP}$
1	$\langle\{V^{\mu\nu}, f_+^{\rho\alpha}\}\nabla_\alpha u^\sigma\rangle$
2	$\langle\{V^{\mu\alpha}, f_+^{\rho\sigma}\}\nabla_\alpha u^\nu\rangle$
3	$i\langle\{V^{\mu\nu}, f_+^{\rho\sigma}\}\chi_-\rangle$
4	$i\langle V^{\mu\nu}[f_-^{\rho\sigma}, \chi_+]\rangle$
5	$\langle\{\nabla_\alpha V^{\mu\nu}, f_+^{\rho\alpha}\}u^\sigma\rangle$
6	$\langle\{\nabla_\alpha V^{\mu\alpha}, f_+^{\rho\sigma}\}u^\nu\rangle$
7	$\langle\{\nabla^\sigma V^{\mu\nu}, f_+^{\rho\alpha}\}u_\alpha\rangle$

Table 1. Odd-intrinsic parity operators with a vector resonance V, a vector current J and a light pseudoscalar, P. The common factor $\varepsilon_{\mu\nu\rho\sigma}$ is omitted in all operators.

where the ideal ω-ϕ mixing scheme (in which $\omega = \sqrt{\frac{2}{3}}\omega_8 + \frac{1}{\sqrt{3}}\omega_0$) has been used, as obtained in the large-N_C limit. The kinetic terms for the V resonances read

$$\mathcal{L}_V^{\rm Kin} = -\frac{1}{2}\langle\nabla_\lambda V^{\lambda\nu}\nabla^\rho V_{\rho\nu}\rangle + \frac{1}{4}M_V^2\langle V_{\mu\nu}V^{\mu\nu}\rangle - e_m^V\langle V_{\mu\nu}V^{\mu\nu}\chi_+\rangle\,, \tag{2.11}$$

where a common U(3)-symmetric mass, M_V, appears. It is corrected by the e_m^V-term, yielding a pattern according to phenomenology [129, 130]. We note that interactions are hidden in the expansion of the covariant derivatives above, but these play no rôle in our work. We turn now to the relevant interactions involving at least one vector resonance field.

Operators with one vector resonance field.

We start with the even-intrinsic parity sector, where we have

$$\mathcal{L}_V^{\rm even} = \frac{F_V}{2\sqrt{2}}\langle V_{\mu\nu}f_+^{\mu\nu}\rangle + \frac{\lambda_V}{\sqrt{2}}\langle V_{\mu\nu}\{f_+^{\mu\nu}, \chi_+\}\rangle\,, \tag{2.12}$$

with the first term giving the leading contribution to the V^0-γ coupling and the second one including its flavor-symmetry breaking correction, proportional to quark masses.[9]

In the odd-intrinsic parity sector one has

$$\mathcal{L}_V^{\rm odd} = \sum_{j=1}^{7}\frac{c_j}{M_V}\mathcal{O}^j_{VJP}\,, \tag{2.13}$$

where the complete list of operators contributing to our processes of interest (via φ-γ-V vertices) is collected in table 1. Among these operators only $\mathcal{O}^3_{VJP}$ breaks chiral symmetry[10](the others will also give flavor-breaking contributions for real φs, once their wave functions renormalizations and mixings are accounted for; with similar comments applying below).

Operators with two vector resonance fields.

These contributions are of the following type:

$$\mathcal{L}_{VV}^{\rm odd} = \sum_{j=1}^{4} d_j\mathcal{O}^j_{VVP}\,, \tag{2.14}$$

[9]We note that $\lambda_V = \sqrt{2}\lambda_6^V$ in ref. [128].

[10]Although $\mathcal{O}^4_{VJP}$ also breaks chiral symmetry, its contribution vanishes for the processes studied here.

JHEP12(2024)203

j	$\mathcal{O}^j_{VV'P}$
a	$\langle\{V^{\mu\nu}, V'^{\rho\alpha}\}\nabla_\alpha u^\sigma\rangle$
b	$\langle\{V^{\mu\alpha}, V'^{\rho\sigma}\}\nabla_\alpha u^\nu\rangle$
c	$\langle\{\nabla_\alpha V^{\mu\nu}, V'^{\rho\alpha}\}u^\sigma\rangle$
d	$\langle\{\nabla_\alpha V^{\mu\alpha}, V'^{\rho\sigma}\}u^\nu\rangle$
e	$\langle\{\nabla^\sigma V^{\mu\nu}, V'^{\rho\alpha}\}u_\alpha\rangle$
f	$i\langle\{V^{\mu\nu}, V'^{\rho\sigma}\}\chi_-\rangle$

Table 2. Odd-intrinsic parity operators with one vector meson resonance, one excited vector meson resonance, and a pseudo-Goldstone boson [131]. A common $\varepsilon_{\mu\nu\rho\sigma}$ factor is omitted in all operators.

where the only relevant operators in our case are (the common factor $\varepsilon_{\mu\nu\rho\sigma}$ is omitted)

$$\mathcal{O}^1_{VVP} = \langle\{V^{\mu\nu}, V^{\rho\alpha}\}\nabla_\alpha u^\sigma\rangle\,, \quad \mathcal{O}^2_{VVP} = i\langle\{V^{\mu\nu}, V^{\rho\sigma}\}\chi_-\rangle\,, \quad \mathcal{O}^3_{VVP} = \langle\{\nabla_\alpha V^{\mu\nu}, V^{\rho\alpha}\}u^\sigma\rangle\,. \tag{2.15}$$

Among these, $\mathcal{O}^2_{VVP}$ breaks unitary flavor symmetry.

Operators with excited vector resonance fields.

For the second vector multiplet, V', we repeat all operators that we had for the first one, V. That is, we add eqs. (2.10) to (2.15)) for the excited vector mesons. In this way, we will have the new parameters (denoted by a prime) $M_{V'}, e_m^{V'}, F_{V'}, \lambda_{V'}, \{c'_i\}_{i=1}^7, \{d'_j\}_{j=1}^3$.

Additionally, we will also have new $VV'P$ interactions, which are [131]

$$\mathcal{L}^{\rm odd}_{VV'} = \sum_{j=a,b,c,d,e,f} d_j \mathcal{O}^j_{VV'P}\,, \tag{2.16}$$

with the $\mathcal{O}^j_{VV'P}$ shown in table 2.

Operators with pseudoscalar resonance fields.

The pseudoscalar resonances, P' (with analogous flavor structure to the φ mesons), give subleading contributions via their mixing with the lightest pseudo-Goldstones, φ, that are suppressed as $m_P^2/m_{P'}^2$. However, the P' multiplet is crucial to recover the QCD-ruled short-distance behaviour on the VVP Green's function [122, 138]. Because of this, we must also take into consideration the pieces

$$\begin{aligned}\Delta\mathcal{L}^{\rm even}_P &= \frac{1}{2}\langle\nabla_\mu P'\nabla^\mu P'\rangle + i d_m\langle P'\chi_-\rangle\,,\\ \Delta\mathcal{L}^{\rm odd}_P &= \varepsilon_{\mu\nu\rho\sigma}\langle\kappa_5^P\,\{f_+^{\mu\nu}, f_+^{\rho\sigma}\}\,P' + \kappa_3^{PV}\,\{V^{\mu\nu}, f_+^{\rho\sigma}\}\,P' + \kappa^{PVV}V^{\mu\nu}V^{\rho\sigma}P'\rangle\,,\end{aligned} \tag{2.17}$$

which need to be repeated for $V \to V'$. The operator with coefficient $d_m^{(\prime)}$ vanishes in the chiral limit.

There will also be a $VV'P'$ operator [132],

$$\Delta\mathcal{L}^{\rm odd}_{VV'P'} = \kappa^{VV'P'}\langle\{V^{\mu\nu}, V'^{\mu\nu}\}P'\rangle\,, \tag{2.18}$$

that we need to include for consistency.

JHEP12(2024)203

We will briefly comment next on the flavor breaking induced by our $\mathcal{L}_{\mathrm{R}\chi\mathrm{T}}$, eq. (2.1), in the resonance sector,[11] where we account for $\mathcal{O}(m_P^2)$ corrections in interaction vertices, resonance masses and field renormalizations [124].

The e_m^V contribution, cf. eq. (2.11), yields the following pattern of masses for the lightest non-strange neutral vector mesons

$$M_\rho^2 = M_\omega^2 = M_V^2 - 4e_m^V m_\pi^2\,, \quad M_\phi^2 = M_V^2 - 4e_m^V \Delta_{2K\pi}^2\,, \tag{2.19}$$

with $\Delta_{2K\pi} = 2m_K^2 - m_\pi^2$. Analogous relations are obtained for the V' multiplet. We will work under the simplifying assumption that their flavor structure is analogous, so that $e_m^{V'} = e_m^V \frac{M_{V'}^2}{M_V^2}$. The similar shifts for the P' mesons will not be needed, as the induced corrections are subleading, namely $\mathcal{O}(m_P^4)$. Our cutting of the infinite tower of resonances per set of quantum numbers that are predicted in the large-N_C limit to a few of them implies that the $N_C \to \infty$ masses get shifted as a result. Consequently, the masses will be used as free fit parameters and will not be fixed to their physical values. The uncertainty on $a_\mu^{\mathrm{HLbL-pole}}$ associated to cutting the infinite spectrum to a few of the lightest states cannot be large, but it will anyway be relevant at the current level of precision. The main reason lies in the kernel needed to evaluate this contribution to the $g_\mu - 2$, that is strongly dominated by the $[0.1, 1]\,\mathrm{GeV}^2$ region (for both photon virtualities), providing $\sim 85\%$ of the full results. This is considered in the assessment of theory uncertainties of our RχT approach in section 7.1.

The V^0-γ transitions will be shifted due to the λ_V term in eq. (2.12). This will imply the following changes

$$(\rho^0/\omega) - \gamma : F_V \to F_V + 8m_\pi^2 \lambda_V\,, \quad \phi - \gamma : F_V \to F_V + 8\Delta_{2K\pi}^2 \lambda_V\,, \tag{2.20}$$

with an analogous primed version for the V'^0-γ vertices.

3 Transition form factors in RχT

The most general transition amplitude between an on-shell $P = \pi^0/\eta/\eta'$ meson and two generally off-shell photons with virtualities (polarizations) $q_1^2(\epsilon_1^*)$ and $q_2^2(\epsilon_2^*)$ is

$$\mathcal{M}_{P\gamma^*\gamma^*} = ie^2 \varepsilon^{\mu\nu\rho\sigma} q_{1\mu} q_{2\nu} \epsilon_{1\rho}^* \epsilon_{2\sigma}^* \mathcal{F}_{P\gamma^*\gamma^*}(q_1^2, q_2^2)\,, \tag{3.1}$$

which is given in terms of the P transition form factor $\mathcal{F}_{P\gamma^*\gamma^*}(q_1^2, q_2^2)$, fulfilling $\mathcal{F}_{P\gamma^*\gamma^*}(q_1^2, q_2^2) = \mathcal{F}_{P\gamma^*\gamma^*}(q_2^2, q_1^2)$, due to Bose symmetry under the exchange of the identical photons. This form factor is illustrated in figure 1. There are three types of contributions to $\mathcal{F}_{P\gamma^*\gamma^*}(q_1^2, q_2^2)$: local terms, and one- and two-resonance exchange diagrams, as shown in figure 2.

The different contributions to $\mathcal{F}_{P\gamma^*\gamma^*}(q_1^2, q_2^2)$ considering only one vector resonance multiplet are described minutely in ref. [124], so we will not detail them here. Nonetheless, it is important to quote the redefinition of combinations of the coupling constants appearing

[11] Chiral symmetry breaking in $\mathcal{L}_{\mathrm{no}\ R}$ happens as in χPT.

JHEP12(2024)203

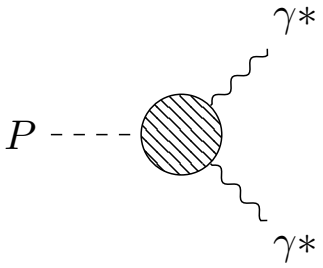

Figure 1. Schematic representation of the $P \to \gamma^*\gamma^*$ ($P = \pi^0, \eta, \eta'$) Transition Form Factor.

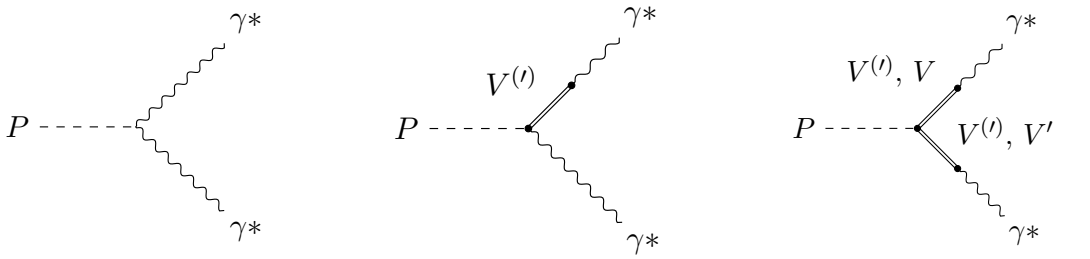

(a) Local. (b) One-resonance exchange. (c) Two-resonances exchange.

Figure 2. Different contributions to the $P\gamma^*\gamma^*$ vertex.

in [124] that will also enter our results:[12]

$$c_{1235} \to c^*_{1235} = c_1 + c_2 + 8c^*_3 - c_5\,, \tag{3.2a}$$

$$d_{123} \to d^*_{123} = d_1 + 8d^*_2 - d_3\,, \tag{3.2b}$$

$$d_{abcf} \to d^*_{abcf} = d_a + d_b - d_c + 8d^*_f\,. \tag{3.2c}$$

The contributions from the second vector multiplet can be obtained by simply adding the same terms with primed couplings. We will concentrate here on the new terms that come from the $VV'P$ contributions to the two-resonances exchange diagrams, like in figure 2(c). After that, we will quote the expressions of the P form factors before requiring short-distance constraints (whence the remaining contributions, can be read off easily).

The contributions coming from $\mathcal{L}_{VV'P}$, eq. (2.16), read

$$\begin{aligned}\mathcal{F}^{VV'P}_{\pi^0\gamma^*\gamma^*}(q_1^2,q_2^2) = \frac{2}{3F_\pi}\Bigg\{&(F_V+8m_\pi^2\lambda_V)(F_{V'}+8m_\pi^2\lambda_{V'})\left(m_\pi^2 d_{abcf}+d_{abc}q_1^2+d_{abcd}q_2^2\right)\\ &\times\left(\frac{1}{(M_\rho^2-q_1^2)(M_{\omega'}^2-q_2^2)}+\frac{1}{(M_{\rho'}^2-q_1^2)(M_\omega^2-q_2^2)}\right)+(q_1\leftrightarrow q_2)\Bigg\}\,,\end{aligned} \tag{3.3}$$

where we defined the combinations of couplings

$$d_{abcf} = d_a + d_b - d_c + 8d_f\,, \quad d_{abc} = d_a - d_b + d_c\,, \quad d_{abcd} = -d_a + d_b + d_c - 2d_d\,, \tag{3.4}$$

[12] This redefinition of coupling constants applies for both vector meson resonance multiplets, so the c's and the d's are also redefined in the same way.

JHEP12(2024)203

and

$$\mathcal{F}^{VV'P}_{\eta\gamma^*\gamma^*}(q_1^2,q_2^2)=\frac{2}{3F}\left\{\left[5C_q\frac{2}{3}(F_V+8m_\pi^2\lambda_V)(F_{V'}+8m_\pi^2\lambda_{V'})\frac{d_{abcf}m_\eta^2+d_{abc}q_1^2+d_{abcd}q_2^2-8d_f\Delta_{\eta\pi}^2}{(M_{\rho'}^2-q_1^2)(M_\rho^2-q_2^2)}\right.\right.$$
$$\left.\left.+(\{5C_q\to-\sqrt{2}C_s,\Delta_{\eta\pi}\to-\Delta_{2K\pi\eta},\rho^{(\prime)}\to\phi^{(\prime)}\})\right]+(q_1\leftrightarrow q_2)\right\}, \tag{3.5}$$

where we introduced $\Delta_{\eta\pi}^2=m_\eta^2-m_\pi^2$ and $\Delta_{2K\pi\eta}^2=2m_K^2-m_\pi^2-m_\eta^2$. The pion wave-function renormalization has changed the global $1/F$ factor to $1/F_\pi$, for $N_C\to\infty$ [140–142], in eq. (3.3). In this equation. there is no ϕ contribution because ideal mixing for the vector meson resonances was used. For the $\eta^{(\prime)}$, ρ,ω,ϕ contribute; however, the isospin symmetry limit leads to $M_{\rho^{(\prime)}}=M_{\omega^{(\prime)}}$ so we have chosen to use $\rho^{(\prime)}$'s mass and propagator only. For the $\eta^{(\prime)}$ cases, the dependencies are on $C_{q/s}^{(\prime)}/F$, which are functions of $\{f,\theta\}_{8/0}$, see eqs. (2.8).

As always, an analogous expression is obtained for $\mathcal{F}_{\eta'\gamma^*\gamma^*}(q_1^2,q_2^2)$ by replacing $C_q\to C_q'$, $C_s\to-C_s'$ and $m_\eta\to m_{\eta'}$, and the $\eta^{(\prime)}$ expressions reduce to the π^0 one in the U(3) flavor symmetry limit. In the chiral limit, our results for the P transition form factors reproduce those in refs. [122, 123]. Neglecting the contributions involving the V' multiplet we recover the results in ref. [124].

Since we want to make use of the short-distance constraints on the VVP Green's function derived in refs. [122, 123], the effect of the pseudoscalar resonance multiplet P' needs to be accounted for. The operator with coefficient d_m (from $\Delta\mathcal{L}_P^{\text{even}}$ in eq. (2.17)) introduces a mixing between the P' and φ states, proportional to quark masses, starting at $\mathcal{O}(m_P^2)$. As a result, the contribution from the P' states can be introduced by simply rescaling couplings as follows [124]:

$$C_7^W\to C_7^{W*}=C_7^W+\frac{4d_m\kappa_5^P}{3M_{P'}}\,, \tag{3.6a}$$

$$c_3\to c_3^*=c_3+\frac{d_mM_V\kappa_3^{PV}}{M_{P'}^2}\,,\ ^{13} \tag{3.6b}$$

$$d_2\to d_2^*=d_2+\frac{d_m\kappa^{PVV}}{2M_{P'}^2}\,, \tag{3.6c}$$

$$d_f\to d_f^*=d_f+\frac{d_m\kappa^{PVV'}}{2M_{P'}^2}\,, \tag{3.6d}$$

where the last redefinition was not proposed before, to our knowledge. The remaining couplings do not need shifting.

4 Short distance constraints

We will demand that our form factors, $\mathcal{F}_{P\gamma^*\gamma^*}(q_1^2,q_2^2)$, $P=\pi^0,\eta,\eta'$, satisfy the high-energy requirements stemming from QCD [148–151]:

$$\lim_{Q^2\to\infty}-Q^2\mathcal{F}_{\pi^0\gamma^*\gamma^*}(-Q^2,-Q^2)=\frac{2F_\pi}{3}\,, \tag{4.1a}$$

[13] A short-distance constraint on κ_3^{PV} was found in ref. [122]. We will not use it, like in ref. [124], as it does no longer hold when the V' and P' multiplets are also considered.

JHEP12(2024)203

$$\lim_{Q^2\to\infty} -Q^2\mathcal{F}_{\pi^0\gamma^*\gamma^*}(-Q^2,0) = 2F_\pi\,, \tag{4.1b}$$

with $q^2=-Q^2$. At leading order in the perturbative expansion, the results for the $\eta^{(\prime)}$ mesons are obtained multiplying those for the π^0, eqs. (4.1), by $\frac{5C_q-\sqrt{2}C_s}{3}$ $\left(\frac{5C'_q+\sqrt{2}C'_s}{3}\right)$, respectively. We comment on α_S and higher-order operator product expansion (OPE) corrections below eq. (4.14).

We will apply these constraints first in the chiral limit, and then including $\mathcal{O}(m_P^2)$ corrections. Our results will be independent of considering corrections at this order to the LO values for the $C^{(\prime)}_{q/s}$ mixing coefficients, so we will keep them unexpanded throughout.

In addition to demanding the leading ultraviolet behaviour in the singly and doubly virtual limits of the transition form factors, we will also require the additional constraints derived from the short-distance analysis of the VVP Green's function. By matching the leading terms of the QCD OPE for infinite virtualities, within the chiral and large-N_C limits, Kampf and Novotny [122] obtain that the following (linear combinations of) constants vanish

$$C_{22}^W = C_7^{W*} = c_{125} = c'_{125} = c_{1235} = c'_{1235} = 0\,, \tag{4.2}$$

where we first used here $c_{125}=c_1-c_2+c_5$. Their remaining results are compatible with our findings that will be detailed next:

- Doubly Virtual π^0-TFF:
  - $\mathcal{O}(Q^0)$, $\mathcal{O}(m_P^0)$:
$$c'_{1256} = -M_{V'}\frac{M_V N_C + 32\sqrt{2}\pi^2 F_V c_{1256}}{32\sqrt{2}\pi^2 F_{V'} M_V}\,, \tag{4.3}$$
    where $c^{(\prime)}_{1256} = c_1^{(\prime)} - c_2^{(\prime)} - c_5^{(\prime)} + 2c_6^{(\prime)}$ appears (primed combinations of constants are defined analogously below).
  - $\mathcal{O}(Q^0)$, $\mathcal{O}(m_P^2)$:
$$\lambda_V = \lambda_{V'} = 0\,. \tag{4.4}$$
  - $\mathcal{O}(Q^{-2})$, $\mathcal{O}(m_P^0)$:
$$c_{1256} = \frac{8d_3F_V + 4d_{abc}F_{V'} - \frac{F_\pi^2 M_V^2}{F_V(M_V^2-M_{V'}^2)}}{4\sqrt{2}M_V}\,. \tag{4.5}$$
  - $\mathcal{O}(Q^{-2})$, $\mathcal{O}(m_P^2)$:
$$c^*_{1235} = -e_m^V\frac{8d_3F_V + 4d_{abc}F_{V'} - \frac{F_\pi^2 M_V^2}{F_V(M_V^2-M_{V'}^2)}}{\sqrt{2}M_V}\,. \tag{4.6}$$
- Singly Virtual π^0-TFF:
  - $\mathcal{O}(Q^0)$, $\mathcal{O}(m_P^0)$:
$$d'_3 = \frac{-M_V^2M_{V'}^2N_C - 32\pi^2 d_{abcd}F_VF_{V'}M_V^2 - 64\pi^2 d_3F_V^2M_{V'}^2 - 32\pi^2 d_{abc}F_VF_{V'}M_{V'}^2}{64\pi^2F_{V'}^2M_V^2}\,. \tag{4.7}$$

JHEP12(2024)203

– $\mathcal{O}(Q^0)$, $\mathcal{O}(m_P^2)$:

$$c_{1235}^{*\prime} = -\frac{M_{V'}}{8\sqrt{2}\pi^2 F_{V'} M_V^4}\Big(-e_m^{V'} M_V^4 N_C - 64\pi^2 d_3 e_m^{V'} F_V^2 M_V^2 - 32\pi^2 d_{abc} e_m^{V'} F_V F_{V'} M_V^2 + 64\pi^2 d_3 e_m^V F_V^2 M_{V'}^2 + 32\pi^2 d_{abc} e_m^V F_V F_{V'} M_{V'}^2 + 8\sqrt{2}\pi^2 c_{1235}^* F_V M_V M_{V'}^2\Big)\,. \tag{4.8}$$

– $\mathcal{O}(Q^{-2})$, $\mathcal{O}(m_P^0)$:

$$d_{abc} = -\frac{-M_V^2 M_{V'}^4 N_C + 4\pi^2[4 d_{abcd} M_V^2 F_V F_{V'}(M_V^2 - M_{V'}^2) + 16 d_3 F_V^2 M_{V'}^2 (M_V^2 - M_{V'}^2) + 5 F_\pi^2 M_V^2 M_{V'}^2]}{16\pi^2 F_V F_{V'} M_{V'}^2 (M_V^2 - M_{V'}^2)}\,. \tag{4.9}$$

– $\mathcal{O}(Q^{-2})$, $\mathcal{O}(m_P^2)$:

$$d_{123}^{\prime *} = -\frac{F_V[2 d_{123}^* F_V M_{V'}^2 + d_{abcf}^* F_{V'}(M_V^2 + M_{V'}^2)]}{2 F_{V'}^2 M_V^2}\,. \tag{4.10}$$

We note that the relation $e_m^{V'} = e_m^V \frac{M_{V'}^2}{M_V^2}$, which stems from our assumption of identical flavor structure for the V and V' nonets, precisely cancels the $\mathcal{O}(Q^0)$, $\mathcal{O}(m_P^4)$ terms in the singly virtual asymptotic limit (in fact they are cancelled to all orders in m_P^2). We anyway recall that our computation only retains $\mathcal{O}(m_P^2)$ corrections.

We find additional constraints, coming from either the η or η' form factors, which are:

- Doubly Virtual η-TFF:

  – $\mathcal{O}(Q^0)$,$\mathcal{O}(m_P^0)$:

  $$C_8^W = 0\,. \tag{4.11}$$

  – $\mathcal{O}(Q^{-2})$,$\mathcal{O}(m_P^2)$:

  $$c_3^* = e_m^V \frac{16\pi^2 d_{abcd} F_V F_{V'} M_V^2 (M_V^2 - M_{V'}^2) + 32\pi^2 d_3 F_V^2 M_{V'}^2 (M_V^2 - M_{V'}^2) + 24\pi^2 F_\pi^2 M_V^2 M_{V'}^2}{32\sqrt{2}\pi^2 F_V M_V M_{V'}^2 (M_V^2 - M_{V'}^2)}\,. \tag{4.12}$$

- Singly Virtual η-TFF:

  – $\mathcal{O}(Q^0)$,$\mathcal{O}(m_P^2)$:

  $$c_3^{\prime *} = \frac{M_{V'}^3\left(\sqrt{2} e_m^V M_V N_C - 128\pi^2 c_3^* F_V\right)}{128\pi^2 F_{V'} M_V^3}\,. \tag{4.13}$$

  – $\mathcal{O}(Q^{-2})$,$\mathcal{O}(m_P^2)$:

  $$d_2^{\prime *} = -\frac{F_V[2 d_2^* F_V M_{V'}^2 + d_f^* F_{V'}(M_V^2 + M_{V'}^2)]}{2 F_{V'}^2 M_V^2}\,. \tag{4.14}$$

We remark that our setting provides π^0, η, η' transition form factors which, in the chiral limit, follow the proportionality $1 : \frac{5C_q - \sqrt{2}C_s}{3} : \frac{5C_q' + \sqrt{2}C_s'}{3}$. This implies that it is not able to accommodate the corrections to eqs. (4.1) due to the anomalous dimension of the singlet

JHEP12(2024)203

axial current [152], which are relevant for the $\eta^{(\prime)}$ cases. Our fit results, however, will not hint to any need for improving on this point presently. Higher order corrections to the first of eqs. (4.1) have been computed using the OPE, and multiply it by $\left(1-\frac{8}{9}\frac{\delta_P^2}{Q^2}\right)$. For the π^0, $\delta_\pi^2 = 0.20(2)\,\text{GeV}^2$, determined from QCD sum rules [149]. For the $\eta^{(\prime)}$ the corresponding values have not been computed, although it is reasonable to expect that they deviate from the π^0 result by typical U(3) (and large-N_C) breaking corrections, $\lesssim 30\%$ [22].

Our short-distance constraints on the RχT parameters are compatible with those found in $\tau^- \to P^-[\gamma]\nu_\tau$ [153–155] and $\tau^- \to (VP)^-\nu_\tau$ decays [156]. They are consistent with those derived studying the $\tau^- \to (KK\pi)^-\nu_\tau$ [157] and $\tau^- \to \eta^{(\prime)}\pi^-\pi^0\nu_\tau$ [158] decays provided $F_V = \sqrt{3}F$ [138], a relation that is also favored in $\tau^- \to (\pi\pi\pi)^-\nu_\tau$ decays [159–161], which is driven by the axial-vector current.

We will not quote the $\mathcal{F}_{P\gamma^*\gamma^*}$ form factors obtained after applying the short-distance constraints discussed previously, but after employing the next definitions. First, we introduce the following barred couplings:[14]

$$\bar{d}_{123} = \frac{F_V^2}{3F_\pi^2} d^*_{123}\,, \tag{4.15a}$$

$$\bar{d}_{abcf} = \frac{F_V F_{V'}}{6F_\pi^2} d^*_{abcf}\,, \tag{4.15b}$$

$$\bar{d}_2 = \frac{F_V^2}{3F_\pi^2} d^*_2\,, \tag{4.15c}$$

$$\bar{d}_f = \frac{F_V F_{V'}}{6F_\pi^2} d^*_f\,, \tag{4.15d}$$

$$\bar{d}_3 = \frac{F_V^2}{3F_\pi^2} d_3. \tag{4.15e}$$

Further, the dependence of our results on $\bar{d}_{123}(\bar{d}_2)$ and $\bar{d}_{abcf}(\bar{d}_f)$ suggests us to introduce their following convenient combinations

$$d_{s1} = \left(1-\frac{M_V^2}{M_{V'}^2}\right)\left(\bar{d}_{abcf} + \frac{M_{V'}^2}{M_V^2}\bar{d}_{123}\right)\,, \tag{4.16a}$$

$$d_{s2} = \left(1-\frac{M_V^2}{M_{V'}^2}\right)\left(\bar{d}_f + \frac{M_{V'}^2}{M_V^2}\bar{d}_2\right)\,, \tag{4.16b}$$

which appear for single and double virtuality, and

$$d_{d1} = \left(1-\frac{M_{V'}^2}{M_V^2}\right)\left(\bar{d}_{abcf} + \bar{d}_{123}\right)\,, \tag{4.17a}$$

$$d_{d2} = \left(1-\frac{M_{V'}^2}{M_V^2}\right)\left(\bar{d}_f + \bar{d}_2\right)\,, \tag{4.17b}$$

[14] $\bar{d}_{123}$ and $\bar{d}_2$ were already used in ref. [124].

JHEP12(2024)203

that enter only for double virtuality. It is also advantageous to employ

$$d_{d3} = \left(1 - \frac{M_{V'}^2}{M_V^2}\right)^2 \bar{d}_3, \tag{4.18}$$

that is only sensitive to the doubly virtual photon case.

Altogether, this enables to recast the $\mathcal{F}_{P\gamma^*\gamma^*}$ form factors as

$$\begin{aligned}\mathcal{F}_{\pi^0\gamma^*\gamma^*}(q_1^2,q_2^2) = &\Big\{96\pi^2F_\pi^2(m_\pi^2M_\rho^2M_{\rho'}^2d_{s1}+m_\pi^2q_1^2q_2^2d_{d1}+2M_\rho^2q_1^2q_2^2d_{d3})+N_CM_{V'}^2M_{\rho'}^2(q_1^2q_2^2-M_\rho^4)\\ &+4F_\pi^2\pi^2q_1^2q_2^2(q_1^2+q_2^2-2M_\rho^2)+24F_\pi^2\pi^2M_{\rho'}^2\left[(q_1^2+q_2^2)M_\rho^2-2q_1^2q_2^2\right]\Big\}\\ &/\left[24\pi^2F_\pi(M_\rho^2-q_1^2)(M_\omega^2-q_2^2)(M_{\rho'}^2-q_1^2)(M_{\omega'}^2-q_2^2)\right]+(q_1\leftrightarrow q_2),\end{aligned} \tag{4.19}$$

and

$$\begin{aligned}&\mathcal{F}_{\eta\gamma^*\gamma^*}(q_1^2,q_2^2) =\\ &\frac{5C_q}{18F\pi^2(M_\rho^2-q_1^2)(M_\rho^2-q_2^2)(M_{\rho'}^2-q_1^2)(M_{\rho'}^2-q_2^2)}\times\\ &\Big\{\pi^2F_\pi^2\Big[24m_\eta^2d_{s1}M_\rho^2M_{\rho'}^2-192d_{s2}M_\rho^2M_{\rho'}^2\Delta_{\eta\pi}^2+24m_\eta^2q_1^2q_2^2d_{d1}-192q_1^2q_2^2d_{d2}\Delta_{\eta\pi}^2+48q_1^2q_2^2d_{d3}M_\rho^2\\ &-\left(q_1^2q_2^2(2M_\rho^2-q_1^2-q_2^2)+6M_{\rho'}^2\left(2q_1^2q_2^2-M_\rho^2\left(q_1^2+q_2^2\right)\right)\right)\Big]+N_C\left(-\frac{M_{V'}^2}{4}\right)\left(M_{\rho'}^2(M_\rho^4-q_1^2q_2^2)\right)\Big\}\\ &+(q_1\leftrightarrow q_2)+\left(5C_q\to-\sqrt{2}C_s,\rho\leftrightarrow\phi,\rho'\leftrightarrow\phi',\Delta_{\eta\pi}^2\to-\Delta_{2K\eta\pi}^2\right).\end{aligned} \tag{4.20}$$

The η' form factor is obtained by replacing $C_q \to C_q'$, $C_s \to -C_s'$ and $m_\eta \to m_{\eta'}$ in eq. (4.20).

As in the π^0 case (see the related explanation below eq. (3.5)), the $\eta^{(\prime)}$ transition form factors neither depend on the pion decay constant in the chiral limit, F. These are functions of $C_q^{(\prime)}/F$ and $C_s^{(\prime)}/F$, which in turn depend just on the two mixing angles $\theta_{8/0}$ and decay constants $f_{8/0}$, (2.8).

5 Form factor data analysis

We start this section recalling the criteria required in the White Paper for taking an evaluation of $a_\mu^{P-\text{pole,HLbL}}$ into account, before dwelling on the details of our fits to data in section 5.1. These conditions were that (quoting from ref. [4]):

1. in addition to the transition form factor normalization given by the real-photon decay widths, also high-energy constraints must be fulfilled;

2. at least the spacelike experimental data for the singly-virtual TFF must be reproduced;

3. systematic uncertainties must be assessed with a reasonable procedure.

JHEP12(2024)203

As for the doubly-virtual transition form factor, the experimental data is still very scarce as there is only one measurement by BaBar consisting of five data points for the η' transition form factor with relatively large uncertainties. Therefore, we require our doubly-virtual transition form factors to be not only in accord with the BaBar data for the η' but also in line with the Lattice-QCD data released by the Budapest-Marseille-Wuppertal (BMW) collaboration for the π^0, η and η' doubly-virtual TFFs. As in the singly-virtual case, systematic uncertainties must be also assessed reasonably. We suggest that, for the second White Paper, one should demand — in addition to the three points above — consistency between data-driven P TFF and lattice QCD results, particularly for double virtuality, where these constitute now the best input.

5.1 Fit to transition form factors data

We will start recapitulating the parameters dependence of our P transition form factors, eqs. (4.19) and (4.20), with appropriate substitutions for the η' case.

In principle, a couple of parameters are needed to specify the masses within each V multiplet, M_V, e_m^V, and their primed counterparts. However, our assumption of identical flavor structure for both nonets erases the dependence on $e_m^{V'}$. Therefore, the corresponding spectra will be specified by three independent parameters, that we choose to be $M_V, e_m^V, M_{V'}$. In addition to these, we will have the four parameters associated to the $\eta^{(\prime)}$ mixing, our choice being the decay constants and mixing angles $\{f, \theta\}_{8/0}$. The final five fitted parameters will be those specifying the functional dependence for single and double photon virtuality: $d_{s1,d1,d3}$ for $P = \pi^0$ and also $d_{s2,d2}$ for the $\eta^{(\prime)}$, for a total of 12 fitted parameters. Among them, only $M_{V^{(\prime)}}$ and d_{d3} are U(3)-symmetric, while the rest break this flavor symmetry.

Since our focus is on the P-pole contributions to $a_\mu^{\rm HLbL}$, we will only fit spacelike data ($q^2 \leq 0$). The timelike region is more involved within RχT, because resonance widths are needed, which is a next-to-leading order effect in the $1/N_C$ expansion. Although it is phenomenologically clear that this is the leading next-to-leading order effect, other terms at this order may not be negligible and complicate the treatment. Additionally, radiative corrections can be more important in the timelike region [162].

We will use the following data:

- The decay widths $\Gamma(P \to \gamma\gamma)$, corresponding to the transition form factors evaluated for null virtuality (real photons),

$$\Gamma(P \to \gamma\gamma) = \frac{(4\pi\alpha)^2}{64\pi} m_P^3 |\mathcal{F}_{P\gamma\gamma}(0,0)|^2 \,, \tag{5.1}$$

  are helpful in the characterization of the η-η' mixing and constitute the normalization which receives chiral corrections for low virtualities. These inputs are taken from the PDG [143].[15]

- Transition form factor data from the BaBar [163, 164], Belle [165], CELLO [166], CLEO [167] and LEP [168] experiments, for the singly virtual case.

[15] We are not taking $\Gamma(\eta' \to \gamma\gamma)$ as a separate data point, since it uses LEP data that we are fitting, see next item.

JHEP12(2024)203

$Q_1^2 = Q_2^2$ [GeV^2]	0.1	1	4
π^0	0.0194(3)	0.0475(4)	0.0514(12)
0.1	1	0.2758	0.1556
1	0.2758	1	0.1222
4	0.1556	0.1222	1
η	0.0158(11)	0.0440(26)	0.0474(31)
0.1	1	0.6743	0.3006
1	0.6743	1	0.4615
4	0.3006	0.4615	1
η'	0.0251(30)	0.0920(100)	0.0934(114)
0.1	1	0.8658	0.3840
1	0.8658	1	0.4423
4	0.3840	0.4423	1

Table 3. Central values, uncertainties and correlation matrix for the doubly virtual transition for factors, generated at three representative values of $q_1^2 = q_2^2$ from the BMW results [170] and used in our fits.

- There is only one measurement for double virtuality, by BaBar, in the η' channel [169], consisting of five points (which are insufficient to reliably fit our three parameters $d_{d1,d2,d3}$). We will increase the sensitivity to the doubly virtual regime by supplementing BaBar's with Lattice QCD results [170–172]. Specifically, from the z-expansion performed by the BMW collaboration in [170], we generate three points (at $Q_1^2 = Q_2^2 = 0.1\,, 1.0$, and $4.0\,\text{GeV}^2$) for all three P mesons.[16] These points are shown in table 3. We would like to note here that at least the Lattice data for the η doubly-virtual transition form factor shall be included in the fits to obtain a satisfactory simultaneous description of all three mesons.

As in ref. [124], we will take advantage of stabilization points for the fit, using the results from a previous determination of the $\{f, \theta\}_{8/0}$ parameters [144–147, 173, 174][17]

$$\begin{gathered}\theta_8 = (-21.2 \pm 1.6)^\circ\,, \quad \theta_0 = (-9.2 \pm 1.7)^\circ, \\ f_8 = (1.26 \pm 0.04) F_\pi = (116.2 \pm 3.7)\text{MeV}, f_0 = (1.17 \pm 0.03) F_\pi = (107.9 \pm 2.8)\text{MeV}\,,\end{gathered} \tag{5.2}$$

which increase the χ^2 by barely more than unit.

[16] Given that the z-expansion has 6 parameters (with their corresponding correlation) one can generate at most 6 points for having an invertible covariance matrix. Four our analysis, we only generate 3 *lattice* points for each P to avoid high correlations between (neighboring) points [143]. We note that 3 is the minimum number of points we need to fix the three doubly virtual parameters. Had we used 4, 5 or 6 data points we would have obtained highly correlated data, which implies a (close to) non-invertible covariance matrix, that over-represents the lattice information.

[17] The correlation between the fitted parameters describing the singly and doubly virtual behavior (now $d_{s1,s2,d1,d2}$) and $\{f, \theta\}_{8/0}$ is large, like with a single vector resonance multiplet (as in ref. [124]), which calls for adding these extra fit points in order to keep the fit within the physical region.

JHEP12(2024)203

The fits can compensate for the neglected higher V excitations by shifting any of the mass parameters M_V or M'_V. We choose to keep M_ρ close to its PDG value by adding it as a point in the cost function.

We will add to the χ^2 a final fit point, corresponding to $\delta_\pi^2 = 0.20(2)\,\text{GeV}^2$ (see the discussion below eq. (4.14)).

The cost function for this fit will then be:

$$\chi^2_{\text{Global}} = \chi^2_{\pi^0_{\text{SV}}} + \chi^2_{\eta_{\text{SV}}} + \chi^2_{\eta'_{\text{SV}}} + \chi^2_{\pi^0_{\text{DV}}} + \chi^2_{\eta_{\text{DV}}} + \chi^2_{\eta'_{\text{DV}}} + \sum_{P}^{\text{ExtraPoints}} \left(\frac{P_{\text{exp}} - P_{\text{model}}}{\Delta P_{\text{exp}}} \right)^2 , \tag{5.3}$$

which includes the transition form factor data for single and double virtuality, SV and DV (where the latter incorporate lattice input) for the P channels, and the extra points given by: the $\Gamma(P \to \gamma\gamma)$ decay widths [143], the decay constants and mixing angles of the $\eta - \eta'$ system (5.2), M_ρ [143], and $\delta_\pi^2 = 0.20(2)\,\text{GeV}^2$ [149].

Regarding the Lattice data, the correlations between the generated data were also considered in each of the $\chi^2_{P^{\text{LQCD}}_{DV}}$, so their contribution to the reduced χ^2 in eq. (5.3) is given by:

$$\chi^2_{P^{\text{LQCD}}_{DV}} = \sum_{i,j=1}^{3} \left(P_i^{\text{LQCD}} - P_i^{\text{R}\chi\text{T}} \right) \left(\text{Cov}_{ij}^{\text{LQCD}} \right)^{-1} \left(P_j^{\text{LQCD}} - P_j^{\text{R}\chi\text{T}} \right) , \tag{5.4}$$

where $P^{\text{LQCD}}_{i(j)}$ and $\left(\text{Cov}^{\text{LQCD}}_{ij}\right)^{-1}$ are, respectively, the central value and the inverse of the covariance matrix of the lattice data given in table 3.[18]

Following previous analyses of the $\mathcal{F}_{P\gamma^*\gamma^*}$ form factors and their contributions to a_μ^{HLbL} [42, 123, 124, 175–187] and owing to our preliminary fits for this work, we will not include BaBar π^0 data in our reference fit, as it is inconsistent with Belle's, that appears more compatible with the predicted (Brodsky-Lepage) asymptotic limit.[19] Additionally, the chiral symmetry relations among the different P form factors data points at the largest measured energies are best satisfied without the BaBar π^0 data. The uncertainty associated to the reliability of the latter is assessed in section 7.1.

Our preliminary fits show a big correlation (close to one) of the pairs of parameters $\{d_{s1}, d_{s2}\}$ and $\{d_{d1}, d_{d2}\}$. This motivates us to consider instead their combinations

$$d_{s1} = \langle d_{s1} \rangle + \frac{\sigma_{d_{s1}}}{\sqrt{2}} \left(\sqrt{1+r_s}\, r_{s1} - \sqrt{1-r_s}\, r_{s2} \right) , \tag{5.5a}$$

$$d_{s2} = \langle d_{s2} \rangle + \frac{\sigma_{d_{s2}}}{\sqrt{2}} \left(\sqrt{1+r_s}\, r_{s1} + \sqrt{1-r_s}\, r_{s2} \right) , \tag{5.5b}$$

and analogously for the doubly virtual case ($s \to d$), in order to minimize their correlations (assuming small interdependences with the rest of the parameters, which is a good approximation). Eqs. (5.5) use the mean values of the preliminary fit ($\langle d_{s1} \rangle, \langle d_{s2} \rangle$) and their uncertainties ($\sigma_{d_{s1}}, \sigma_{d_{s2}}$). The new parameters are r_{s1}, r_{s2}, defined through the original correlation $r_s \sim 1$ (same with $s \to d$).

[18] Taking the covariance matrix into account introduces extra degrees of freedom due to having non-diagonal entries different from zero equal. The additional d.o.f. equal the non redundant entries of the covariance matrix.

[19] We have checked that the fits are worse if these BaBar data is kept, like in ref. [124].

JHEP12(2024)203

Parameter	Fit Result
M_V [GeV]	0.752(2)
e_m^V	-0.32(4)
$M_{V'}$ [GeV]	1.933(4)
r_{s1}	0.0(0.6)
r_{s2}	0.0(0.9)
r_s	0.9976
$\langle d_{s1}\rangle$	-1.6(6)
$\langle d_{s2}\rangle$	-0.21(7)
θ_8 [°]	-18.5(6)
θ_0 [°]	-6.9(1.6)
f_8 [MeV]	118.8(4)
f_0 [MeV]	99.4(1.7)
r_{d1}	0.0(0.5)
r_{d2}	0.0(0.9)
r_d	0.9783
$\langle d_{d1}\rangle$	-2.8(2.0)
$\langle d_{d2}\rangle$	-0.31(24)
d_{d3}	-3.48(3)
χ^2_{Global}/d.o.f.	148.0/110

Table 4. Our best fit results, with uncertainties in parentheses. The input values of the rotations (5.5) are also given, where the errors in the $\langle d\rangle$ are the σ_d's.

	M_V	e_m^V	$M_{V'}$	r_{s1}	r_{s2}	θ_8	θ_0	f_8	f_0	r_{d1}	r_{d2}	d_{d3}
M_V	1	0.739	−0.035	0.501	−0.065	0.035	−0.008	−0.077	−0.025	0.357	−0.152	0.371
e_m^V	0.739	1	−0.106	0.614	−0.120	−0.009	0.019	−0.099	−0.053	0.300	−0.145	0.344
$M_{V'}$	−0.035	−0.106	1	−0.035	−0.114	−0.032	0.202	0.063	−0.030	−0.446	0.399	−0.837
r_{s1}	0.501	0.614	−0.035	1	0.226	0.335	0.029	−0.014	−0.113	0.217	−0.097	0.186
r_{s2}	−0.065	−0.120	−0.114	0.226	1	0.185	−0.219	0.089	0.431	0.026	0.211	0.082
θ_8	0.035	−0.009	−0.032	0.335	0.185	1	0.002	−0.657	−0.069	0.075	0.071	0.015
θ_0	−0.008	0.019	0.202	0.029	−0.219	0.002	1	−0.001	0.605	−0.069	−0.041	−0.187
f_8	−0.077	−0.099	0.063	−0.014	0.089	−0.657	−0.001	1	0.032	−0.047	0.002	−0.084
f_0	−0.025	−0.053	−0.030	−0.113	0.431	−0.069	0.605	0.032	1	−0.011	0.165	0.030
r_{d1}	0.357	0.300	−0.446	0.217	0.026	0.075	−0.069	−0.047	−0.011	1	−0.152	0.140
r_{d2}	−0.152	−0.145	0.399	−0.097	0.211	0.071	−0.041	0.002	0.165	−0.152	1	−0.392
d_{d3}	0.371	0.344	−0.837	0.186	0.082	0.015	−0.187	−0.084	0.030	0.140	−0.392	1

Table 5. Correlation matrix between the 12 fitted parameters of the best fit.

Our best fit results corresponding to the minimization of the cost function (5.3) are given in table 4 with the correlation matrix shown in table 5. The comparison of our $\mathcal{F}_{P\gamma^*\gamma^*}(q_1^2, q_2^2)$ to data for single and double virtuality are displayed in figures 3 and 4.

We will comment now on the big correlations that can still be seen in table 5. The redefinition in eq. (4.18) shows that we cannot make any further rotation of parameters to avoid the anticorrelation of −0.837 between M_V' and d_{d3}.[20] We rotated the parameters

[20] Besides, the correlation between them is non-linear, so we could not proceed analogously.

JHEP12(2024)203

d_{s1} and d_{s2}, according to eq. (3.6), to minimize their correlation. We note that the rotated parameter r_{s1} has big correlations with both M_V and e_m^V (which is not the case for its partner rotated parameter, r_{s2}). Correlations between the η-η' mixing parameters are slightly larger than in ref. [124], but still reasonable. The large correlation between M_V and e_m^V is entirely a result of fixing M_ρ to its PDG value. In our preliminary fits, floating both parameters independently, their correlation was only ~ 0.22.

We will discuss next the central values of our reference fit:

- M_V is typically smaller than the results obtained in single resonance approximations ($\sim 800\,\text{MeV}$ [151, 188]) but the value of $M_{\rho(\phi)}$ is still compatible, at 1(2) σ, with the PDG [143].

- As commented above, e_m^V is highly correlated with M_V because we are requiring that $M_V^2 - 4e_m^V m_\pi^2 \sim M_\rho^2$, cf. eq. (2.19). Nevertheless, the value of this flavor symmetry breaking parameter is compatible at less than one standard deviation with the best fit result in ref. [124].

- One should not expect $M_{V'}^2 - 4e_m^{V'} m_\pi^2 \sim M_{\rho'}^2$, because $M_{V'}^2$ (we recall that we are assuming $e_m^{V'} M_V^2 = e_m^V M_{V'}^2$) absorbs the effect of the neglected higher V excitations, so its fitted value $M_{V'} \sim 1.933\,\text{GeV}$ appears reasonable.

- Concerning the η-η' mixing parameters, agreement of our fitted values with the input (5.2) is acceptable, with differences being $1.2(0.70)\sigma$ for $\theta_{8(0)}$, and $0.4(1.9)\sigma$ for $f_{8(0)}$.

- For our best fit values, eq. (4.18) implies that $d_{d3} \sim 30\bar{d}_3$, with $\bar{d}_3 \sim d_3$. Short-distance QCD constraints on the VVP Green's function [122, 138] determine $d_3 \sim -0.126$, corresponding to a d_{d3} with a deviation of less than 10% from our best fit value.

- Best fit values for the parameters $r_{s1,s2}$ and $r_{d1,d2}$ are compatible with zero. Little information is known on the couplings of the V' multiplet that enter the definition of the original couplings $d_{s1,s2}$ and $d_{d1,d2}$. If we set them to zero for a rough estimate and take into account that $\bar{d}_{123,2} \sim d_{123,2}$, we can use that $d_{123} \sim 1/24$ [122, 138] (again from the short-distance behaviour of the VVP Green's function), to estimate that $d_{s1} \sim 1/4$ and $d_{d1} \sim 5/4$, which agree within 1 and 3σ with our best fit. According to refs. [189–192] $d_2 = 0.08 \pm 0.08$, that again yields estimates d_{s2} and d_{d2} in agreement with our best fit results.

The comparison of the transition form factors corresponding to our best fit results (table 4) to data in the singly virtual regime for the π^0, η and η' mesons in figure 3 is very satisfactory but for a few points that seem to be outliers, given the general trend shown by the data. At the largest measured virtualities our transition form factors seem to approach faster the Brodsky-Lepage limit than the data, that have large uncertainties there, anyway.

An analogous comparison for double virtuality is shown in figure 4, where the relevance of the lattice data is evident -these data are extremely helpful in our analysis to constrain the doubly-virtual parameters $d_{d1,d2,d3}$. We note that a couple of low-energy points in the $\eta\,(\eta')$ case are below (above) our curves, although the statistical significance of this tension is

JHEP12(2024)203

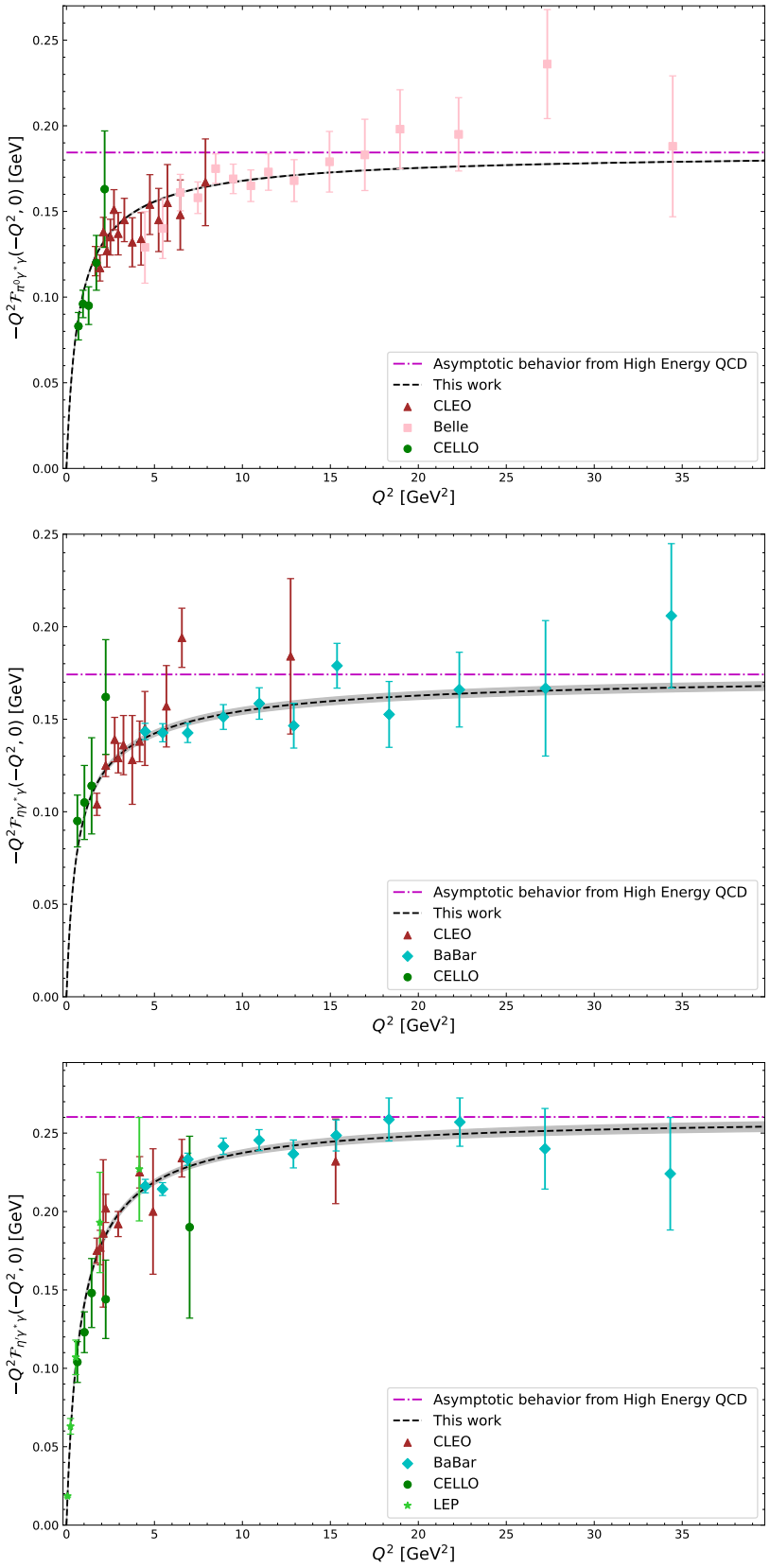

Figure 3. The transition form factors corresponding to our best fit results (table 4) are compared to data in the singly virtual regime for π^0, η and η'. We do not show BaBar data for the π^0 case [163], which was not used in our reference fits.

JHEP12(2024)203

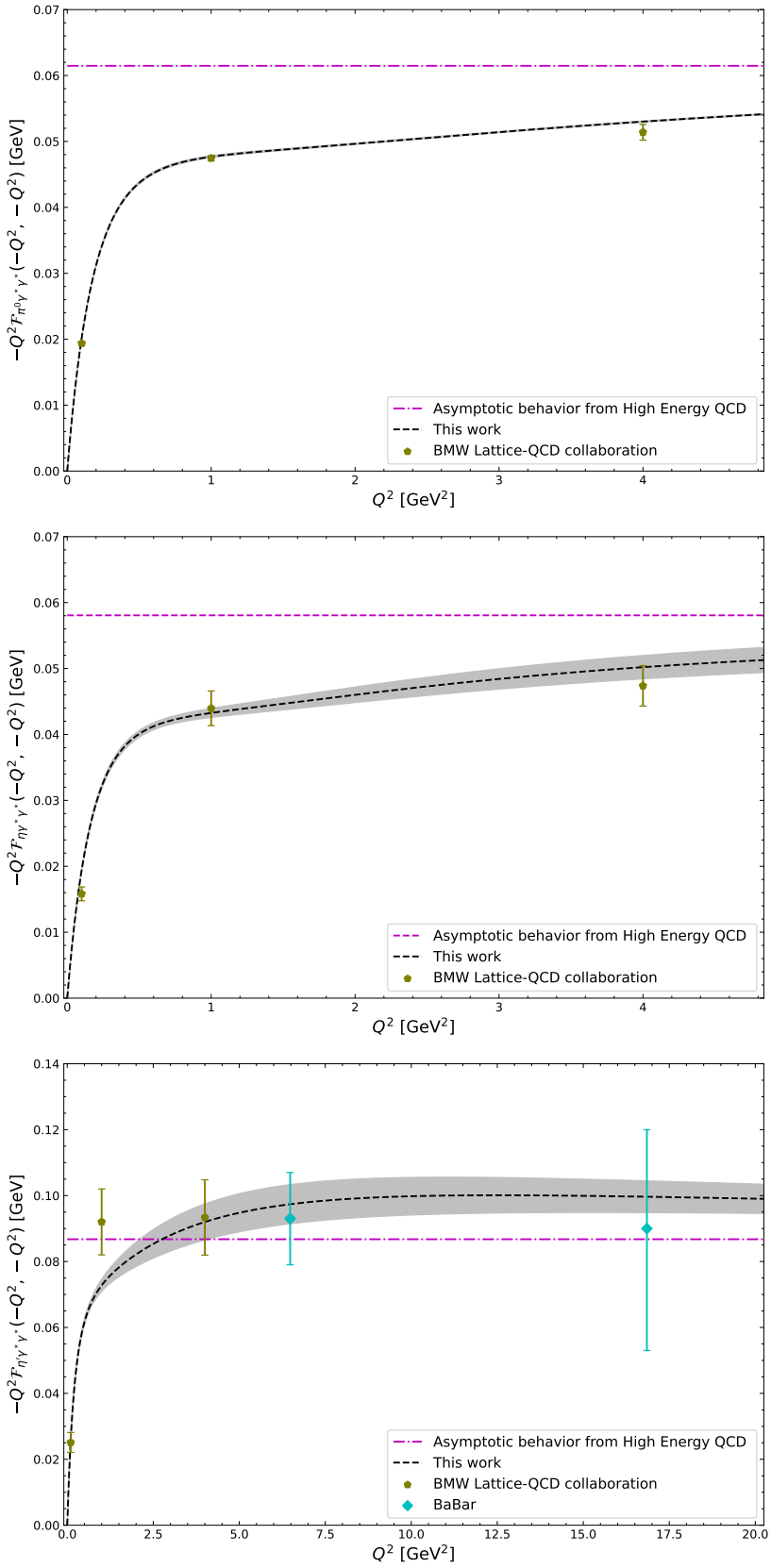

Figure 4. The transition form factors corresponding to our best fit results (table 4) are compared to data in the doubly virtual regime for π^0, η and η'.

JHEP12(2024)203

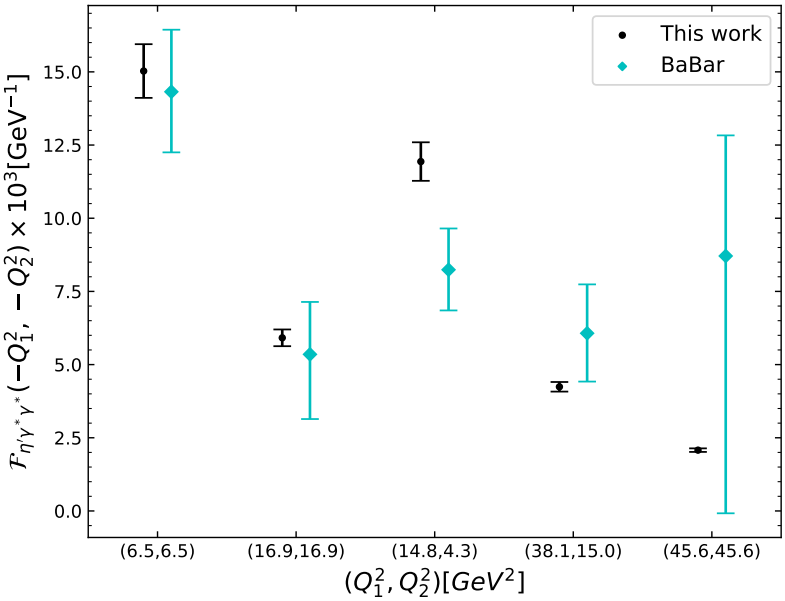

Figure 5. BaBar data (cyan diamonds) for the η' doubly-virtual transition form factor [169] as compared to our best fit results (black circles) from table 4.

moderate. As a sanity check, we have verified that the comparison of our best fit results to lattice QCD exhibits a similar pattern in the singly virtual case.[21] In addition, in figure 5 we show a comparison of the standalone BaBar measurements of the η' doubly-virtual transition form factor, which includes non-diagonal Q^2 data points, together with our best fit results. As seen, the results are in good agreement, while the experimental statistics is not sufficiently precise yet as to further constrain the parameters of double virtuality.

We have extracted the slope parameters, $\{b, c, d\}_P$, defined from

$$\lim_{Q^2\to 0} \mathcal{F}_{P\gamma^*\gamma}(-Q^2, 0) = \mathcal{F}_{P\gamma\gamma}(0,0)\left(1 - \frac{b_P}{m_P^2}Q^2 + \frac{c_P}{m_P^4}Q^4 - \frac{d_P}{m_P^6}Q^6 + \cdots\right), \tag{5.6}$$

corresponding to our best fit results, and compare them to ref. [22] in table 6. Like this reference, we do not quote our results for d_π, because the sensitivity of the data and our fit to this parameter is very small, because of chiral suppression. The agreement for b_P (and for c_π) is very good while the accord with the other parameters shown is quite satisfactory. In the last row for each channel, we recall the coefficient of the $\mathcal{O}(1/Q^2)$ term in the single asymptotic (Brodsky-Lepage) limit (P_∞), see eq. (6.4b), for which both analyses agree within one standard deviation.

Finally, it is important to remark that, besides having reproduced the Short-Distance Constraints (SDC) for all 3 particles and having a good agreement with other descriptions at intermediate energies, the decay widths $\Gamma(P \to \gamma\gamma)$ are also in great agreement with the experimental values -we have obtained a value of 7.67(9) eV for π^0 (which is a 0.6σ

[21] We cannot add these data to our fit since they would be double counted (they are obtained from the double virtuality data, setting one photon on-shell). We could have decided to use this information for the singly virtual case, but it was much more useful to employ it for double virtuality in our case, as we did.

JHEP12(2024)203

Parameter	Our result	Values in [22]	Difference between both
b_π	0.03163(16)	0.0321(19)	0.2σ
c_π	0.000862(6)	0.00104(22)	0.8σ
π_∞	$2F_\pi$	$2F_\pi$	0σ
b_η	0.600(10)	0.572(8)	1.6σ
c_η	0.316(7)	0.333(9)	1.1σ
d_η	0.164(4)	0.195(20)	1.3σ
η_∞[GeV]	0.174(3)	0.180(12)	0.4σ
$b_{\eta'}$	1.26(2)	1.31(3)	1.0σ
$c_{\eta'}$	1.86(4)	1.74(9)	0.9σ
$d_{\eta'}$	2.82(6)	2.30(22)	1.9σ
η'_∞[GeV]	0.260(4)	0.255(4)	0.6σ

Table 6. Low-energy slope parameters $\{b, c, d\}_P$ and Brodsky-Lepage parameter (P_∞) from our best fit result and their comparison with the values used in [22].

difference with respect to [193, 194]), 497(13) eV for the η (0.6σ difference with [195]) and 4.3(2) KeV for η' (0.2σ difference with [168]). This agreement is noteworthy, given the slight tension (in the π^0 and η cases) between the lattice QCD results for these widths and the PDG values (see also our footnote 13).

6 Equivalence with the Canterbury Approximants

Since the White Paper values [4] for the $\eta^{(\prime)}$-pole contributions to $a_\mu^{\rm HLbL}$ come from the Canterbury Approximants (CA) analysis of ref. [22], we will translate our RχT description including two multiplets of vector resonances to the CA language and comment on the corresponding implications in this section.[22]

CA were successfully used for the description of the transition form factors of the non-strange neutral pseudoscalar mesons π^0, η and η' [22] (see ref. [197] for the extrapolation to the timelike region). They are described by a rational function $f(x, y)$ of polynomials which are analytic, symmetric under $x \leftrightarrow y$ and satisfy the accuracy-through-order conditions [22, 198–202]. A C_M^N is defined then as:

$$C_M^N(x, y) = \frac{R_N(x, y)}{Q_M(x, y)} = \frac{\sum_{i,j=0}^{N} a_{i,j} x^i y^j}{\sum_{i,j=0}^{M} b_{i,j} x^i y^j} \,. \tag{6.1}$$

Ref. [22] mentioned that both $C_{N+1}^N(Q_1^2, Q_2^2)$ and $C_N^N(Q_1^2, Q_2^2)$ work for describing the high-energy behavior prescribed by perturbative QCD [148–151], eqs. (4.1). Choosing one or the other depends on whether dropping the last term(s) of the polynomial from R_N or Q_M in eq. (6.1). Given this constriction, the convergence and Bose symmetry are guaranteed at arbitrary virtualities for both photons. Increasing N and/or M implies incrementing the

[22] Obviously, it is impossible to relate analytically our framework to the dispersive approach [24], which provides the reference result for the π^0 contribution [4]. A dispersive analysis for the $\eta^{(\prime)}$ contributions has recently appeared during the proofreading of this work [196].

JHEP12(2024)203

freedom of the model, so that an optimal choice of them must be done with both freedom and over-fitting in mind. In [22], a C_2^1 was used[23] (we do not write a subscript P in the α and β coefficients in eq. (6.2), although they are different for π^0, η, η'):

$$C_2^1(Q_1^2, Q_2^2) = \frac{\mathcal{F}_{P\gamma\gamma}(0,0)\,(1+\alpha_1(Q_1^2+Q_2^2)+\alpha_{1,1}Q_1^2Q_2^2)}{1+\beta_1(Q_1^2+Q_2^2)+\beta_{1,1}Q_1^2Q_2^2+\beta_2(Q_1^4+Q_2^4)+\beta_{1,2}Q_1^2Q_2^2(Q_1^2+Q_2^2)}. \tag{6.2}$$

The low-energy behavior, given by the $Q_1^2, Q_2^2 \to 0$ expansion [203], is:

$$\begin{aligned}\mathcal{F}_{P\gamma^*\gamma^*}(Q_1^2, Q_2^2) = \mathcal{F}_{P\gamma\gamma}(0,0)\Bigg(1 - \frac{b_P}{m_P^2}(Q_1^2+Q_2^2) + \frac{c_P}{m_P^4}(Q_1^4+Q_2^4) \\ + \frac{a_{P;1,1}}{m_P^4}(Q_1^2Q_2^2) - \frac{d_P}{m_P^6}(Q_1^6+Q_2^6) + \cdots\Bigg),\end{aligned} \tag{6.3}$$

and has been widely studied for all 3 particles (see table VI from [22]). The values of $\mathcal{F}_{P\gamma\gamma}(0,0)$, b_P and c_P, together with the high-energy behavior constraints

$$\lim_{Q^2\to\infty} \mathcal{F}_{P\gamma^*\gamma^*}(Q^2, Q^2) = \frac{P_\infty}{3}\left(\frac{1}{Q^2} - \frac{8}{9}\frac{\delta_P^2}{Q^4}\right) + \mathcal{O}(Q^{-6}), \tag{6.4a}$$

$$\lim_{Q^2\to\infty} \mathcal{F}_{P\gamma^*\gamma}(Q^2, 0) = \frac{P_\infty}{Q^2}, \tag{6.4b}$$

impose 6 restrictions to the form factors in eq. (6.2), leaving only $\alpha_{1,1}$ as a free parameter.[24] However, $\alpha_{1,1}$ could not be fitted therein, since it is sensitive only to the doubly virtual case, for which no data was available by then.[25] Now, there are both experimental data [169] (only for η') and lattice QCD evaluations [170–172] which can be -as we illustrated in this work- used to generate data in order to complete this description. An updated version of the CA study is included in this work, both for its intrinsic interest and for comparing to our results in the previous section.

Our form factors satisfying short-distance QCD constraints, eqs. (4.19) and (4.20) -with trivial changes for $\eta \to \eta'$- correspond to a C_2^2 and a C_4^4 CA, respectively. For the π^0 case the CA coefficients matching our parametrization eq. (4.19) are given in table 7.

We make the following important remarks concerning the results in table 7:

- The C_2^2 model has 4 more parameters than the C_2^1 model used in [22]. However, two of them are zero, consequently the degrees of freedom increase by two.

- By construction, our model based on RχT reproduces the dominant behavior of the transition form factors, but the δ_π^2 is only included as a fit point in the χ^2, as opposed to the C_2^1 case, where it is used to fix a coefficient.

[23] The $F_{P\gamma\gamma}(0,0)$ was factored out to provide with a physical meaning the normalization constant, given $a_0 = b_0 = 1$. Besides, the $\beta_{2,2}$ term was dropped -as commented before- in order to correctly account for the high-energy behavior.

[24] For the $\eta^{(\prime)}$ cases, the asymptotic constraint on P_∞ in eq. (6.4b) was traded by the low-energy one on d_P (we recall there is no sensitivity to it for $P = \pi^0$), see table 6.

[25] In ref. [22] the range for $\alpha_{P\,1,1}$ was taken so as to avoid poles for the $C_2^1(Q_1^2, Q_2^2)$ in the spacelike region.

JHEP12(2024)203

CA Coefficient	RχT result
$F_{\pi^0\gamma\gamma}(0,0)$	$\frac{8d_{s1}F_\pi m_\pi^2}{M_\rho^2 M_{\rho'}^2} - \frac{M_V^2 N_C}{12F_\pi M_\rho^2 \pi^2}$
$\alpha_1^\pi F_{\pi^0\gamma\gamma}(0,0)$	$-\frac{2F_\pi}{M_\rho^2 M_{\rho'}^2}$
$\alpha_{1,1}^\pi F_{\pi^0\gamma\gamma}(0,0)$	$-\frac{4F_\pi}{M_\rho^4 M_{\rho'}^2} + \frac{2F_\pi\left(-M_\rho^2+12d_{d1}m_\pi^2+24d_{d3}M_\rho^2\right)}{3M_\rho^4 M_{\rho'}^4} + \frac{M_V^2 N_C}{12F_\pi \pi^2 M_\rho^6}$
$\alpha_2^\pi F_{\pi^0\gamma\gamma}(0,0)$	0
$\alpha_{1,2}^\pi F_{\pi^0\gamma\gamma}(0,0)$	$-\frac{F_\pi}{3M_\rho^4 M_{\rho'}^4}$
$\alpha_{2,2}^\pi F_{\pi^0\gamma\gamma}(0,0)$	0
β_1^π	$M_\rho^{-2}\left(1+\frac{M_V^2}{M_{V'}^2}\right)$
$\beta_{1,1}^\pi$	$M_\rho^{-4}\left(1+\frac{M_V^2}{M_{V'}^2}\right)^2$
β_2^π	$M_\rho^{-2}M_{\rho'}^{-2}$
$\beta_{1,2}^\pi$	$M_\rho^{-4}M_{\rho'}^{-2}\left(1+\frac{M_V^2}{M_{V'}^2}\right)$
$\beta_{2,2}^\pi$	$M_\rho^{-4}M_{\rho'}^{-4}$

Table 7. Translation of our RχT result, eq. (4.19) to CA, for the π^0.

- The slope parameters from [203] are imposed on the C_2^1 up to c_π. In our case (RχT) they are not imposed, but rather we check (satisfactorily) compatibility with the results for them in ref. [22] of our best fit results (see table 6).

- For our RχT results, in the π^0 case, there are only two independent terms in the denominator of the CA, that we choose as β_1 and β_2. For the η' we have $\beta_{1,2,3,4}$, which are independent. The others can be written as $\beta_{i,j} = \beta_i\beta_j$, so they are not quoted in the following.

- In general, there is only 1 free parameter in C_2^1 (3 for C_2^2) per channel, which can now be fitted to 3 points for the π^0 and η (from lattice), and 8 for the η' (from lattice and the BaBar measurement). In our RχT description there are 12 parameters which were simultaneously fitted to 122 data points[26] in the three channels, from different experiments [163–169] (including PDG [143]) and lattice data, generated from ref. [170].

For the $\eta^{(\prime)}$ cases, working with such a high order CA (C_4^4) is not feasible. For illustrative purposes, we obtained the corresponding CA in the chiral limit, which is a C_2^2. In fact, the same one describes the three cases (π^0, η, η'), provided we factor out the overall $1:(5C_q - \sqrt{2}C_s)/3:(5C_q' + \sqrt{2}C_s')/3$ dependence (c_P). The translation of the chiral limit of our results, eqs. (4.19) and (4.20), to CA is given in table 8.

In our updates of the CA results of ref. [22], to be presented below, we have decided to use the same methodology that was employed in this reference for the π^0 also for the $\eta^{(\prime)}$. That is, we will not trade the constraint on P_∞ (Brodsky-Lepage) by the one on d_P

[26] We included eight additional stabilization points, see the paragraphs before eq. (5.3).

JHEP12(2024)203

CA Coefficient	Chiral THS coefficient
$F_{P\gamma\gamma}(0,0)$	$-\frac{c_P N_C}{12 F_\pi \pi^2}$
$\alpha_1 F_{P\gamma\gamma}(0,0)$	$-\frac{2 c_P F_\pi}{M_V^2 M_{V'}^2}$
$\alpha_{1,1} F_{P\gamma\gamma}(0,0)$	$c_P \left(\frac{16 \bar{d}_3 F_\pi (M_V^2 - M_{V'}^2)^2}{M_V^6 M_{V'}^4} + \frac{-\frac{8 F_\pi^2 (M_V^2 + 6 M_{V'}^2)}{M_{V'}^4} + \frac{N_C}{\pi^2}}{12 F_\pi M_V^4} \right)$
$\alpha_2 F_{P\gamma\gamma}(0,0)$	0
$\alpha_{1,2} F_{P\gamma\gamma}(0,0)$	$-\frac{c_P F_\pi}{3 M_V^4 M_{V'}^4}$
β_1	$\left(\frac{1}{M_V^2} + \frac{1}{M_{V'}^2} \right)$
β_2	$\frac{1}{M_V^2 M_{V'}^2}$

Table 8. Translation of the chiral limit of our RχT result, eqs. (4.19) and (4.20), to CA, for $P = \pi^0, \eta, \eta'$.

for $P = \eta^{(\prime)}$.[27] We will also consider the fits using C_2^2 enforcing the constraints that ensure that no poles be generated in the spacelike region.

Therefore, in this section we will be comparing the following fits to data:

- Our best fit result, described in section 5.1, dubbed RχT below.
- The results obtained considering the chiral limit of eqs. (4.19) and (4.20), which correspond to a C_2^2 CA, as indicated in table 8. This is christened χRχT in what follows.
- The update of the results in ref. [22], using a C_2^1. In this case we change their procedure for the $\eta^{(\prime)}$ cases, as explained in the previous paragraph.
- The fit with a C_2^2,[28] demanding that no poles are generated in the unphysical region. This has also been done using the results in table 8 to determine the C_2^2.

The results of these fits are shown in table 9. According to them, the best agreement with data is obtained for RχT, and only C_2^2 yields fits with a reduced $\chi^2/\text{dof} \sim 1$ as well. Figures 6 and 7 extend figures 3 and 4 by adding the C_2^2 results. In the doubly virtual case, figure 7, it is clear that there are very few points to fit the three coefficients that are independent for each pseudoscalar in C_2^2, causing all 3 pseudoscalar mesons to have the parameter β_{22}^P at limit; consequently, there are poles within the 1σ region of these parameterizations of the TFFs. On the contrary, the 3 couplings sensitive to double virtuality in RχT are related by flavor symmetry, so they are fitted to 14 data points, which prevents overfitting.

[27] We decided to do this because it is consistent with the RχT procedure, see the comparison in table 6. We have checked that proceeding in complete analogy to ref. [22] yields slightly larger χ^2 in the best fit results.

[28] This was performed as a minimal extension of the work in [22], with the same procedure of the update previously described. As mentioned before, this model has 3 free parameters sensitive exclusively to double virtuality data.

JHEP12(2024)203

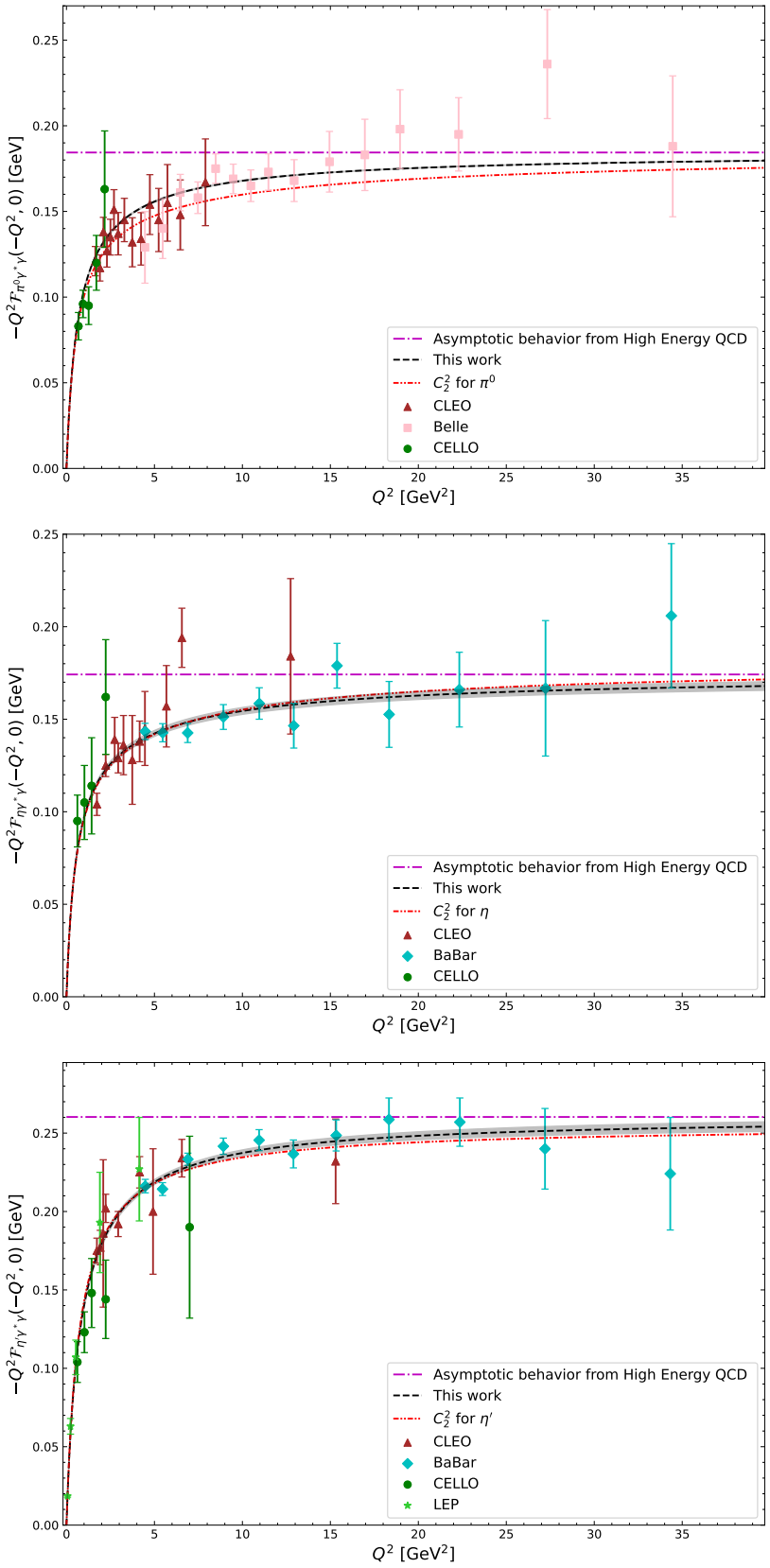

Figure 6. The comparison between our best fit (table 4) for RχT and the C_2^2 results in the singly virtual regime for π^0, η and η'.

JHEP12(2024)203

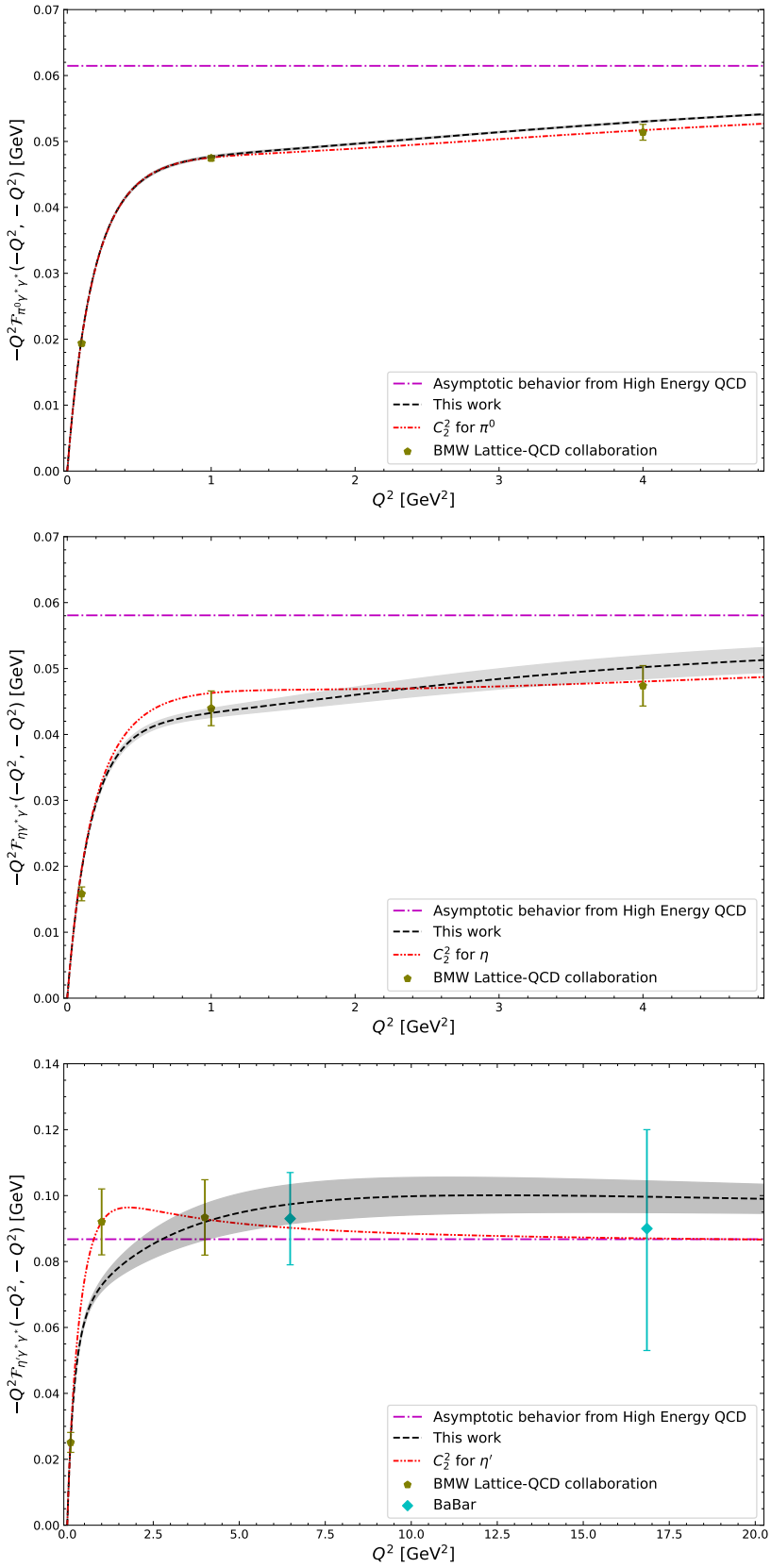

Figure 7. The comparison between our best fit (table 4) for RχT and the C_2^2 results in the doubly virtual regime for π^0, η and η'.

JHEP12(2024)203

Particle	$\chi^2_{\mathrm{R}\chi\mathrm{T}}$/dof	$\chi^2_{\chi\mathrm{R}\chi\mathrm{T}}$/dof	$\chi^2_{C_2^1}$/dof	$\chi^2_{C_2^2}$/dof
π^0	33.3/39	58.2/40	234.0/40	35.18/38
η	47.7/27	61.6/29	63.0/31	44.9/29
η'	50.3/36	208.5/38	42.39/40	33.6/38

Table 9. Our best fit (section 5.1) and its chiral limit are compared to the results obtained using CA. In the C_2^1, case we obtained $a_{P;1,1} = 0.0048(9), 0.75(13), 2.677(25)$ for $P = \pi^0, \eta, \eta'$, respectively.

7 π^0, η, η'-pole contributions to a_μ

In this section we quote the results of our evaluation of the $\pi^0/\eta/\eta'$-pole contributions to the hadronic light-by-light piece of the muon anomalous magnetic moment, $a_\mu^{P\text{-pole, HLbL}}$.[29] We have computed the $a_\mu^{P\text{-pole}}$ contributions according to ref. [204]:

$$a_\mu^{P\text{-pole}} = -\frac{2\alpha^3}{3\pi^2}\int_0^\infty dQ_1 dQ_2 \int_{-1}^1 dt\sqrt{1-t^2}Q_1^3Q_2^3\left[F_1P_6I_1(Q_1,Q_2,t) + F_2P_7I_2(Q_1,Q_2,t)\right], \tag{7.1}$$

where α is the fine structure constant, $Q_i = |Q_i|$, $t = \cos\theta$, $P_6 = \frac{1}{Q_2^2+m_\pi^2}$, $P_7 = \frac{1}{Q_3^2+m_\pi^2}$, $Q_3^2 = Q_1^2 + Q_2^2 + 2Q_1Q_2t$ and the $I_{1(2)}(Q_1,Q_2,t)$ are given in [204]. The information of the transition form factors is encoded in:

$$F_1 = \mathcal{F}_{P\gamma^*\gamma^*}(Q_1^2,Q_3^2)\mathcal{F}_{P\gamma^*\gamma}(Q_2^2,0)\,. \tag{7.2a}$$

$$F_2 = \mathcal{F}_{P\gamma^*\gamma^*}(Q_1^2,Q_2^2)\mathcal{F}_{P\gamma^*\gamma}(Q_3^2,0)\,. \tag{7.2b}$$

In table 10 we collect different recent evaluations of $a_\mu^{P\text{-poles}}$, including ours.[30] We implemented a numerical evaluation, using the VEGAS algorithm [206, 207]. For the computation of the statistical error, we generated 1000 sets of points in the parameter space from a normal multivariate distribution, given the central values and correlations from tables 4 and 5, which were used for the determination of the mean and standard deviation of each $a_\mu^{\mathrm{P-pole}}$.

We summarize the most important differences between our treatment and the other recent RχT analysis [126] in table 11. The approaches followed in earlier studies [122–124] were already introduced in section 1.

7.1 Assessment of systematic theory uncertainties

In the following, we will evaluate here the error on $a_\mu^{P\text{-poles}}$ associated to our RχT description of the P-TFF. Specifically, we will consider the one stemming from the use of different data sets (whether including/excluding BaBar π^0 single virtual data in the global fit), the one coming from cutting the infinite tower of V and P states to two multiplets, the one arising from neglecting subleading corrections in the large-N_C expansion and, finally, the one

[29] In order to lighten the notation, we shall suppress from this point forward the superscript HLbL in a_μ, *i.e.*, we will take $a_\mu^{P\text{-pole, HLbL}} \to a_\mu^{P\text{-pole}}$.

[30] Very recently, the RBC/UKQCD Lattice collaboration has presented a preliminary value for the π^0-pole, $a_\mu^{\pi^0\text{-pole}} = 57.8(1.9)_{\mathrm{stat}}(1.0)_{\mathrm{syst}} \times 10^{-11}$ [205], while the values of $a_\mu^{\eta\text{-pole}} = 14.64(77) \times 10^{-11}$ and $a_\mu^{\eta'\text{-pole}} = 13.44(70) \times 10^{-11}$ [196] have been reported for the η/η'-poles in a dispersive approach.

JHEP12(2024)203

π^0	η	η'	Ref.	Method
$63.0^{+2.7}_{-2.1}$	-	-	[24, 208]	Dispersive
63.6 ± 2.7	16.3 ± 1.4	14.5 ± 1.9	[22]	CA
62.6 ± 1.3	15.8 ± 1.2	13.3 ± 0.9	[119]	Dyson-Schwinger eqs.
61.4 ± 2.1	14.7 ± 1.9	13.6 ± 0.8	[120]	Dyson-Schwinger eqs.
$63.0^{+2.7}_{-2.1}$	16.3 ± 1.4	14.5 ± 1.9	[4]	WP Data-driven
62.3 ± 2.3	-	-	[4, 25]	WP Lattice
57.8 ± 2.0	11.6 ± 2.0	15.7 ± 4.3	[170]	Lattice
61.7 ± 2.0	13.8 ± 5.5	-	[171, 172]	Lattice
63.5 ± 0.8	-	-	[126]	RχT, 3 resonance multiplets
61.9 ± 0.6	15.2 ± 0.5	14.2 ± 0.7	This work	RχT, 2 resonance multiplets

Table 10. Different recent evaluations of $a_\mu^{P\text{-poles}}$, $P = \pi^0, \eta, \eta'$, multiplied by 10^{11}. In the first rows we collect the results quoted in the WP [4]. The last rows include later results. Our uncertainties are only statistical. Our systematic theory errors are assessed in the remainder of this section.

ref. [126]	This work
Ansätze	Computation from the RχT Lagrangian
3 resonance multiplets	2 resonance multiplets
Chiral Limit	Chiral symmetry breaking up to $\mathcal{O}(m_P^2)$
Only π^0 (for which the chiral limit works quite well)	π^0, η, η'
More subleading OPE constraints	Only δ_π as subleading OPE constraint
2019 Lattice data [25]	2023 Lattice data [170]
Only data used	BaBar π^0 data not used

Table 11. Summary of the main differences between our study and ref. [126].

coming from excluding the Lattice QCD data for the doubly virtual TFF in our fits. We have verified that other corrections (from e.g. neglecting higher-order terms in m_P^2, modifying the η-η' mixing parameters according to the NNLO U(3) χPT fit to lattice data of ref. [209], etc.) are negligible with respect to these (see also the related discussion in ref. [124], our relative errors on them are very similar to those reported therein).[31] Although its associated uncertainty is also negligible, we end this section discussing the asymptotic behaviour for asymmetric double virtualities.

Use of all available experimental data. There are several data sets for the P-TFF. Analyses in the literature differ by including/excluding some experimental data or imposing cuts to the fitted data. In this work, as in ref. [124], BaBar data for the single virtual region of π^0 was excluded for the aforementioned reasons in the global fit of the three channels. An estimation of the error induced by this decision was computed by comparing the evaluation of the $a_\mu^{P\text{-pole}}$ obtained by including or excluding these data. The obtained difference for

[31] Also negligible are the uncertainties associated to either using π^0 Lattice data from ref. [25] or [170], and to including or not additional subleading OPE constraints (see table 11).

JHEP12(2024)203

each pseudoscalar meson is:

$$\left(\Delta a_\mu^{\pi^0\text{-pole}}\right)_{\text{Data Sets}} = +0.20 \times 10^{-11}, \tag{7.3a}$$

$$\left(\Delta a_\mu^{\eta\text{-pole}}\right)_{\text{Data Sets}} = -0.02 \times 10^{-11}\,, \tag{7.3b}$$

$$\left(\Delta a_\mu^{\eta'\text{-pole}}\right)_{\text{Data Sets}} = +0.02 \times 10^{-11}\,. \tag{7.3c}$$

As expected, the induced error occurs mainly in the evaluation of $a_\mu^{\pi^0\text{-pole}}$; however, small deviations are present for η and η' because RχT connects the TFFs of the 3 particles trough chiral symmetry.

Finite number of resonances. Even though the full RχT has an infinite tower of resonances, cutting to a finite number is required for practical use (unless there exists an exact resummation mechanism, which usually only happens for the simplest toy models). This analysis includes -besides the pseudo-Goldstone bosons P- two resonance multiplet states for the vector mesons V, V', and one for the pseudoscalar mesons P'. A minimal extension to this model was performed earlier in ref. [126] -referred as three-multiplet resonance-, where a third V'' and P'' were included, albeit in the chiral limit, and only for the π^0 meson.

An estimation of the systematic error caused by having a finite number of resonances was performed using the results from this three-multiplet resonance model and a fit to the data of our model in the chiral limit, χRχT. In ref. [126], the value of $a_\mu^{\pi^0\text{-pole}}$ was computed using the π^0 lattice data from ref. [25] up to $Q^2 = 4\text{GeV}^2$ to fit their free parameters, so an equivalent analysis (with the same dataset) was performed in χRχT to fit the 3 free parameters of table 8 -with the mixing parameters fixed to the results of our best fit — using only the π^0 lattice data points from ref. [170]. For η and η', there is no computation of the pole contributions to the HLbL piece of a_μ, so we cast the overall c_P flavor-space-rotation factor (defined just above table 8) to compute a fair estimate on these contributions within the three-multiplet resonance model. The resulting differences for each particle are:

$$\left(\Delta a_\mu^{\pi^0\text{-pole}}\right)_{\text{finite spectrum}} = +1.8 \times 10^{-11}\,, \tag{7.4a}$$

$$\left(\Delta a_\mu^{\eta\text{-pole}}\right)_{\text{finite spectrum}} = +1.0 \times 10^{-11}\,, \tag{7.4b}$$

$$\left(\Delta a_\mu^{\eta'\text{-pole}}\right)_{\text{finite spectrum}} = +1.4 \times 10^{-11}\,. \tag{7.4c}$$

Subleading corrections in $1/N_C$. We have considered the contributions at leading order in the large-N_C expansion in our computation. We have estimated the impact of neglected higher-order effects by considering the modification to the ρ propagator coming from pion and kaon loops at next-to-leading order (NLO).[32] Although a proper analysis of the SD behavior for the TFF should be done, we will use the result from the electromagnetic form

[32]We have computed this modification up to 1 GeV. At higher energies other effects arise (like, e.g. those associated to inelasticities), with a relevant interplay to this one, need to be accounted for as well.

JHEP12(2024)203

factor of the pion [210], which will amount to the following replacement (the ρ propagator remains real in the whole space-like region, $q^2 < 0$)

$$M_\rho^2 - q^2 \to M_\rho^2 - q^2 + \frac{q^2 M_\rho^2}{96\pi^2 F_\pi^2}\left(A_\pi(q^2) + \frac{1}{2}A_K(q^2)\right), \tag{7.5}$$

where

$$A_P(q^2) = \ln\frac{m_P^2}{M_\rho^2} + 8\frac{m_P^2}{q^2} - \frac{5}{3} + \sigma_P^3(q^2)\ln\left(\frac{\sigma_P(q^2)+1}{\sigma_P(q^2)-1}\right), \tag{7.6}$$

with $\sigma_P(q^2) = \sqrt{1 - \frac{4m_P^2}{q^2}}$. We will take its absolute value (there are other types of corrections at this order that we are disregarding, like those to the VVP vertex, that can have either sign) as the one standard deviation uncertainty induced by missing subleading corrections in the large-N_C limit. Then, we will have:

$$\left(\Delta a_\mu^{\pi^0\text{-pole}}\right)_{1/N_C} = \pm 1.5 \times 10^{-11}, \tag{7.7a}$$

$$\left(\Delta a_\mu^{\eta\text{-pole}}\right)_{1/N_C} = \pm 0.5 \times 10^{-11}, \tag{7.7b}$$

$$\left(\Delta a_\mu^{\eta'\text{-pole}}\right)_{1/N_C} = \pm 0.3 \times 10^{-11}. \tag{7.7c}$$

Combination of experimental and Lattice data. Finally, we evaluate the uncertainty on $a_\mu^{P\text{-poles}}$ that comes from neglecting Lattice QCD data in our fits. In this way, we quantify the difference between a fully data-driven analysis and a hybrid one. The differences, for every P, are:

$$\left(\Delta a_\mu^{\pi^0\text{-pole}}\right)_{\text{Hybrid analysis}} = +0.4 \times 10^{-11}, \tag{7.8a}$$

$$\left(\Delta a_\mu^{\eta\text{-pole}}\right)_{\text{Hybrid analysis}} = -0.6 \times 10^{-11}, \tag{7.8b}$$

$$\left(\Delta a_\mu^{\eta'\text{-pole}}\right)_{\text{Hybrid analysis}} = -0.8 \times 10^{-11}. \tag{7.8c}$$

The π^0-pole increases while the η/η'-poles decrease by including the Lattice data. To the best of our knowledge, this is the first quantification of the difference between a hybrid and a fully data-driven analysis and it is possible here due to chiral symmetry, since the parameters d_{d1}, d_{d2} and d_{d3} appear in the π^0, η and η' TFFs -even though the experimental data is available only for η', a joint description for all the 3 particles can be obtained. This situation contrasts with the case of the Canterbury Approximants analysis presented in table 9, where Lattice data cannot be excluded for π^0 nor for η.

Asymptotic behavior for asymmetric double virtualities. Furthermore, in this work we have imposed the single virtual and symmetric double virtual SDCs, (4.1). However, from the light-cone expansion [151, 177, 211], the SDCs at leading order in pQCD and at leading-twist are given for general large asymmetric virtualities, by:

$$\lim_{Q_{1(2)}^2\to\infty} \mathcal{F}_{P\gamma^*\gamma^*}(-Q_1^2, -Q_2^2) = \frac{P_\infty}{3}\int_0^1 dx \frac{\phi_P(x)}{xQ_1^2 + (1-x)Q_2^2}, \tag{7.9}$$

JHEP12(2024)203

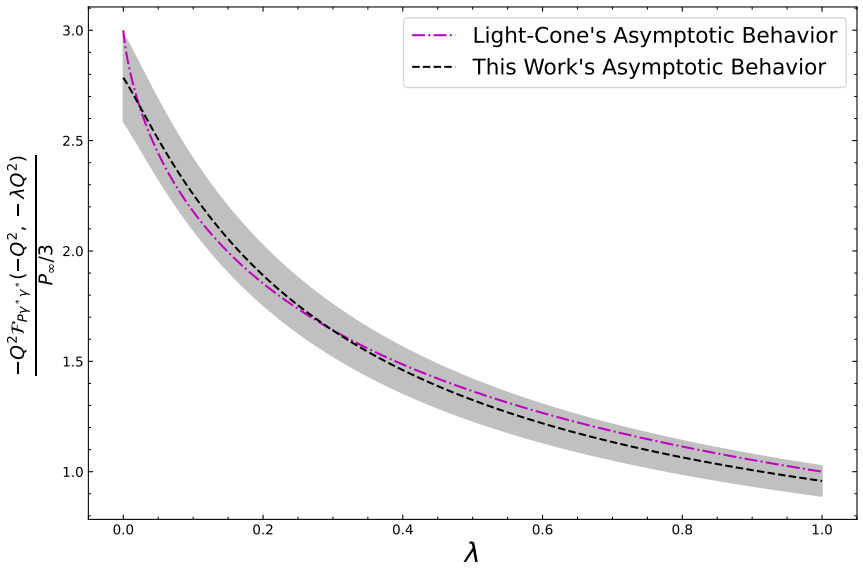

Figure 8. Comparison between the asymptotic behavior of the light-cone expansion and this work's TFFs in terms of the ratio between the 2 squared momenta $\lambda = Q_1^2/Q_2^2$. Our one σ uncertainties are represented by the gray band.

where $\phi_P(x)$ is the pion distribution amplitude which -for large momenta- behaves as $\phi_P(x) \to 6x(1-x)$ [151, 212]. The construction of the TFFs using RχT is limited to a polynomial description, which cannot reproduce the whole range of asymmetries in eq. (7.9). The asymmetric SDCs, $\lim_{Q^2\to\infty} \mathcal{F}_{P\gamma^*\gamma^*}(-Q^2, -\lambda Q^2)$, were compared -for $R\chi T$ and the light-cone expansion results- within the relevant region of the integration kernels for the $a_\mu^{\text{P-pole}}$, as it is shown in figure 8. There is a change in the concavity in the asymptotic behavior of eqs. (4.19) and (4.20) because the term reproducing the symmetric double virtual SDC of eq. (4.1) dominates the whole scale of asymmetries except for $\lambda \to 0$, and it behaves as $1/\lambda$, the effect is more visible at very high energies.

To quantify the effect in the evaluation of $a_\mu^{\text{P-pole}}$ produced by this difference, a replacement of the dominant terms at high energies of eqs. (4.19) and (4.20)) by the one of eq. (7.9) -as suggested in eq. (5.13) from [24]- was done, and the numerical difference was one order of magnitude smaller than the rest of the theory errors for the 3 pseudoscalar mesons. The change for the expression of the light-cone expansion was performed at a Q_1 where the squared difference between this work's asymptotic behavior and eq. (7.9) is minimized.

7.2 Final results with statistical and systematic errors

With the four (independent) dominant uncertainties given by eqs. (7.3), (7.4), (7.7) and (7.8), we obtain the following systematic theory error:

$$\left(\Delta a_\mu^{\pi^0\text{-pole}}\right)_{\text{theory}} = \binom{+2.4}{-1.5} \times 10^{-11}\,, \tag{7.10a}$$

$$\left(\Delta a_\mu^{\eta\text{-pole}}\right)_{\text{theory}} = \binom{+1.1}{-0.8} \times 10^{-11}\,, \tag{7.10b}$$

$$\left(\Delta a_\mu^{\eta'\text{-pole}}\right)_{\text{theory}} = \binom{+1.4}{-0.9} \times 10^{-11}\,. \tag{7.10c}$$

JHEP12(2024)203

Our final result, including statistical (cf. table 10) and the above systematic uncertainties[33] is:

$$a_\mu^{\pi^0\text{-pole}} = \left(61.9 \pm 0.6^{+2.4}_{-1.5}\right) \times 10^{-11} = \left(61.9^{+2.5}_{-1.6}\right) \times 10^{-11}\,, \tag{7.11a}$$

$$a_\mu^{\eta\text{-pole}} = \left(15.2 \pm 0.5^{+1.1}_{-0.8}\right) \times 10^{-11} = \left(15.2^{+1.2}_{-0.9}\right) \times 10^{-11}\,, \tag{7.11b}$$

$$a_\mu^{\eta'\text{-pole}} = \left(14.2 \pm 0.7^{+1.4}_{-0.9}\right) \times 10^{-11} = \left(14.2^{+1.6}_{-1.1}\right) \times 10^{-11}\,, \tag{7.11c}$$

with an uncertainty saturated by the model-dependence. Combining eqs. (7.11a), (7.11b) and (7.11c) we arrive at the following result for the pseudoscalar-pole contributions:

$$a_\mu^{\pi^0+\eta+\eta'\text{-pole}} = \left(91.3 \pm 1.0^{+3.0}_{-1.9}\right) \times 10^{-11} = \left(91.3^{+3.2}_{-2.1}\right) \times 10^{-11}\,. \tag{7.12}$$

8 Conclusions

In this work, we have presented a simultaneous description of the singly and doubly virtual π^0, η and η' transition form factors based on Resonance Chiral Theory that complies with the White Paper consensus agreement for taking their a_μ^{HLbL} contribution into account. In particular, we have shown that working within the two resonance multiplets saturation scheme we: satisfy leading (and some subleading) chiral and high-energy QCD constraints; get a normalization given by the two-photon partial decay width, $\Gamma(\pi^0/\eta/\eta' \to \gamma\gamma)$, that is fully compatible with experimental values; reproduce the singly virtual transition form factors experimental data in the spacelike region (see figure 3) and, last but not least; obtain a faithful description of the doubly virtual transition form factor for all three pseudoscalar mesons resulting from the use of the BaBar data in the η' channel in combination with Lattice-QCD results for the three mesons form factors (see figure 4). Our evaluation of the pole contributions to the hadronic light-by-light piece of the muon $g-2$ read: $a_\mu^{\pi^0\text{-pole}} = \left(61.9 \pm 0.6^{+2.4}_{-1.5}\right) \times 10^{-11}$, $a_\mu^{\eta\text{-pole}} = \left(15.2 \pm 0.5^{+1.1}_{-0.8}\right) \times 10^{-11}$ and $a_\mu^{\eta'\text{-pole}} = \left(14.2 \pm 0.7^{+1.4}_{-0.9}\right) \times 10^{-11}$, for a total of $a_\mu^{\pi^0+\eta+\eta'\text{-pole}} = \left(91.3 \pm 1.0^{+3.0}_{-1.9}\right) \times 10^{-11}$, where the first error is statistical and the second one is systematic (see section 7.1).

Our determination for $a_\mu^{\pi^0\text{-pole}}$ fulfills the quality criteria outlined above being compatible at the level of 1σ with the dispersive evaluation, $a_\mu^{\pi^0\text{-pole}} = \left(63.0^{+2.7}_{-2.1}\right) \times 10^{-11}$ [4] and with the results based on Canterbury approximants, $a_\mu^{\pi^0\text{-pole}} = 63.6(2.7) \times 10^{-11}$ [22], and with the most recent lattice QCD results, $a_\mu^{\pi^0\text{-pole}} = 57.8(2.0) \times 10^{-11}$ [170],[34] and $a_\mu^{\pi^0\text{-pole}} = 61.7(2.0) \times 10^{-11}$ [172]. Our outcomes for the $a_\mu^{\eta/\eta'\text{-pole}}$ contributions are particularly relevant, given that our approach complies with the leading asymptotic behavior for double virtuality and the good performance exhibited for describing the best doubly-virtual input at disposal. Interestingly enough, they are consistent with $a_\mu^{\eta/\eta'\text{-pole}} = [16.3(1.4)/14.5(1.9)] \times 10^{-11}$ from Canterbury Approximants [22], which however would need a C_4^4 to fully account for chiral symmetry constraints and their explicit breaking at leading order, that is non-negligible for the $\eta^{(\prime)}$ contributions (see section 6).[35] Our results are also compatible with the Lattice

[33] We always quote the systematic error after the statistical one.

[34] This result and our work agree within 1.6 σ, which is the biggest among the different works considered, but still reasonable.

[35] At least a C_2^2 would be needed to describe the double virtuality data, instead of the C_2^1 used in ref. [22].

JHEP12(2024)203

results $a_\mu^{\eta/\eta'\text{-pole}} = [11.6(2.0)/15.7(4.2)] \times 10^{-11}$ [170], although the η-pole contribution is in slight tension with our outcome due to the lower value for the normalization of their transition form factor.

We hope that our analysis strengthens the case for experimental measurements of the transition form factors of double virtuality for all three pseudoscalar mesons, as they would allow constraining their functional form and reduce the uncertainty in $a_\mu^{P\text{-pole}}$.

Acknowledgments

The authors are grateful to S. S. Agaev and P. Sánchez-Puertas for useful correspondence and advice and are indebted to the anonymous referee for an insightful report that guided us to polish our manuscript. E. J. E, A. G. and P. R. thank partial funding from Conahcyt (México). E. J. E. also thanks the support of the Inter-American Network of Networks for QCD challenges and of Los Alamos National Laboratory for hospitality -special thanks to E. Mereghetti and S. G-S. for hosting his visit -where the initial stages of this work were developed. The work of S. G-S. is supported by MICIU/AEI/10.13039/501100011033 and by FEDER UE through grants PID2023-147112NB-C21; and through the "Unit of Excellence María de Maeztu 2020-202" award to the Institute of Cosmos Sciences, grant CEX2019-000918-M. Additional support is provided by the Generalitat de Catalunya (AGAUR) through grant 2021SGR01095. S. G-S. is a Serra Húnter Fellow. P. R. acknowledges Conahcyt (México) funding through project CBF2023-2024-3226 as well as Spanish support during his sabbatical through projects MCIN/AEI/10.13039/501100011033, grants PID2020-114473GB-I00 and PID2023-146220NB-I00, and Generalitat Valenciana grant PROMETEO/2021/071.

Data Availability Statement. This article has no associated data or the data will not be deposited.

Code Availability Statement. This article has no associated code or the code will not be deposited.

References

[1] Muon g-2 collaboration, *Final Report of the Muon E821 Anomalous Magnetic Moment Measurement at BNL*, *Phys. Rev. D* **73** (2006) 072003 [hep-ex/0602035] [INSPIRE].

[2] Muon g-2 collaboration, *Measurement of the Positive Muon Anomalous Magnetic Moment to 0.46 ppm*, *Phys. Rev. Lett.* **126** (2021) 141801 [arXiv:2104.03281] [INSPIRE].

[3] Muon g-2 collaboration, *Measurement of the Positive Muon Anomalous Magnetic Moment to 0.20 ppm*, *Phys. Rev. Lett.* **131** (2023) 161802 [arXiv:2308.06230] [INSPIRE].

[4] T. Aoyama et al., *The anomalous magnetic moment of the muon in the Standard Model*, *Phys. Rept.* **887** (2020) 1 [arXiv:2006.04822] [INSPIRE].

JHEP12(2024)203

[5] M. Davier, A. Hoecker, B. Malaescu and Z. Zhang, *Reevaluation of the hadronic vacuum polarisation contributions to the Standard Model predictions of the muon $g-2$ and $\alpha(m_Z^2)$ using newest hadronic cross-section data*, *Eur. Phys. J. C* **77** (2017) 827 [arXiv:1706.09436] [INSPIRE].

[6] A. Keshavarzi, D. Nomura and T. Teubner, *Muon $g-2$ and $\alpha(M_Z^2)$: a new data-based analysis*, *Phys. Rev. D* **97** (2018) 114025 [arXiv:1802.02995] [INSPIRE].

[7] G. Colangelo, M. Hoferichter and P. Stoffer, *Two-pion contribution to hadronic vacuum polarization*, *JHEP* **02** (2019) 006 [arXiv:1810.00007] [INSPIRE].

[8] M. Hoferichter, B.-L. Hoid and B. Kubis, *Three-pion contribution to hadronic vacuum polarization*, *JHEP* **08** (2019) 137 [arXiv:1907.01556] [INSPIRE].

[9] M. Davier, A. Hoecker, B. Malaescu and Z. Zhang, *A new evaluation of the hadronic vacuum polarisation contributions to the muon anomalous magnetic moment and to $\alpha(m_Z^2)$*, *Eur. Phys. J. C* **80** (2020) 241 [*Erratum ibid.* **80** (2020) 410] [arXiv:1908.00921] [INSPIRE].

[10] A. Keshavarzi, D. Nomura and T. Teubner, *$g-2$ of charged leptons, $\alpha(M_Z^2)$, and the hyperfine splitting of muonium*, *Phys. Rev. D* **101** (2020) 014029 [arXiv:1911.00367] [INSPIRE].

[11] A. Kurz, T. Liu, P. Marquard and M. Steinhauser, *Hadronic contribution to the muon anomalous magnetic moment to next-to-next-to-leading order*, *Phys. Lett. B* **734** (2014) 144 [arXiv:1403.6400] [INSPIRE].

[12] Fermilab Lattice et al. collaborations, *Strong-Isospin-Breaking Correction to the Muon Anomalous Magnetic Moment from Lattice QCD at the Physical Point*, *Phys. Rev. Lett.* **120** (2018) 152001 [arXiv:1710.11212] [INSPIRE].

[13] Budapest-Marseille-Wuppertal collaboration, *Hadronic vacuum polarization contribution to the anomalous magnetic moments of leptons from first principles*, *Phys. Rev. Lett.* **121** (2018) 022002 [arXiv:1711.04980] [INSPIRE].

[14] RBC and UKQCD collaborations, *Calculation of the hadronic vacuum polarization contribution to the muon anomalous magnetic moment*, *Phys. Rev. Lett.* **121** (2018) 022003 [arXiv:1801.07224] [INSPIRE].

[15] D. Giusti et al., *Electromagnetic and strong isospin-breaking corrections to the muon $g-2$ from Lattice QCD+QED*, *Phys. Rev. D* **99** (2019) 114502 [arXiv:1901.10462] [INSPIRE].

[16] PACS collaboration, *Hadronic vacuum polarization contribution to the muon $g-2$ with 2+1 flavor lattice QCD on a larger than $(10\,fm)^4$ lattice at the physical point*, *Phys. Rev. D* **100** (2019) 034517 [arXiv:1902.00885] [INSPIRE].

[17] Fermilab Lattice et al. collaborations, *Hadronic-vacuum-polarization contribution to the muon's anomalous magnetic moment from four-flavor lattice QCD*, *Phys. Rev. D* **101** (2020) 034512 [arXiv:1902.04223] [INSPIRE].

[18] A. Gérardin et al., *The leading hadronic contribution to $(g-2)_\mu$ from lattice QCD with $N_f = 2+1$ flavours of O(a) improved Wilson quarks*, *Phys. Rev. D* **100** (2019) 014510 [arXiv:1904.03120] [INSPIRE].

[19] C. Aubin et al., *Light quark vacuum polarization at the physical point and contribution to the muon $g-2$*, *Phys. Rev. D* **101** (2020) 014503 [arXiv:1905.09307] [INSPIRE].

[20] D. Giusti and S. Simula, *Lepton anomalous magnetic moments in Lattice QCD+QED*, *PoS* **LATTICE2019** (2019) 104 [arXiv:1910.03874] [INSPIRE].

JHEP12(2024)203

[21] K. Melnikov and A. Vainshtein, *Hadronic light-by-light scattering contribution to the muon anomalous magnetic moment revisited*, *Phys. Rev. D* **70** (2004) 113006 [hep-ph/0312226] [INSPIRE].

[22] P. Masjuan and P. Sánchez-Puertas, *Pseudoscalar-pole contribution to the $(g_\mu - 2)$: a rational approach*, *Phys. Rev. D* **95** (2017) 054026 [arXiv:1701.05829] [INSPIRE].

[23] G. Colangelo, M. Hoferichter, M. Procura and P. Stoffer, *Dispersion relation for hadronic light-by-light scattering: two-pion contributions*, *JHEP* **04** (2017) 161 [arXiv:1702.07347] [INSPIRE].

[24] M. Hoferichter et al., *Dispersion relation for hadronic light-by-light scattering: pion pole*, *JHEP* **10** (2018) 141 [arXiv:1808.04823] [INSPIRE].

[25] A. Gérardin, H.B. Meyer and A. Nyffeler, *Lattice calculation of the pion transition form factor with $N_f = 2 + 1$ Wilson quarks*, *Phys. Rev. D* **100** (2019) 034520 [arXiv:1903.09471] [INSPIRE].

[26] J. Bijnens, N. Hermansson-Truedsson and A. Rodríguez-Sánchez, *Short-distance constraints for the HLbL contribution to the muon anomalous magnetic moment*, *Phys. Lett. B* **798** (2019) 134994 [arXiv:1908.03331] [INSPIRE].

[27] G. Colangelo et al., *Longitudinal short-distance constraints for the hadronic light-by-light contribution to $(g-2)_\mu$ with large-N_c Regge models*, *JHEP* **03** (2020) 101 [arXiv:1910.13432] [INSPIRE].

[28] V. Pauk and M. Vanderhaeghen, *Single meson contributions to the muon's anomalous magnetic moment*, *Eur. Phys. J. C* **74** (2014) 3008 [arXiv:1401.0832] [INSPIRE].

[29] I. Danilkin and M. Vanderhaeghen, *Light-by-light scattering sum rules in light of new data*, *Phys. Rev. D* **95** (2017) 014019 [arXiv:1611.04646] [INSPIRE].

[30] F. Jegerlehner, *The Anomalous Magnetic Moment of the Muon*, Springer, Cham (2017) [DOI:10.1007/978-3-319-63577-4] [INSPIRE].

[31] M. Knecht, S. Narison, A. Rabemananjara and D. Rabetiarivony, *Scalar meson contributions to a μ from hadronic light-by-light scattering*, *Phys. Lett. B* **787** (2018) 111 [arXiv:1808.03848] [INSPIRE].

[32] G. Eichmann, C.S. Fischer and R. Williams, *Kaon-box contribution to the anomalous magnetic moment of the muon*, *Phys. Rev. D* **101** (2020) 054015 [arXiv:1910.06795] [INSPIRE].

[33] P. Roig and P. Sánchez-Puertas, *Axial-vector exchange contribution to the hadronic light-by-light piece of the muon anomalous magnetic moment*, *Phys. Rev. D* **101** (2020) 074019 [arXiv:1910.02881] [INSPIRE].

[34] G. Colangelo et al., *Remarks on higher-order hadronic corrections to the muon $g-2$*, *Phys. Lett. B* **735** (2014) 90 [arXiv:1403.7512] [INSPIRE].

[35] T. Blum et al., *Hadronic Light-by-Light Scattering Contribution to the Muon Anomalous Magnetic Moment from Lattice QCD*, *Phys. Rev. Lett.* **124** (2020) 132002 [arXiv:1911.08123] [INSPIRE].

[36] T. Aoyama, M. Hayakawa, T. Kinoshita and M. Nio, *Complete Tenth-Order QED Contribution to the Muon $g-2$*, *Phys. Rev. Lett.* **109** (2012) 111808 [arXiv:1205.5370] [INSPIRE].

[37] T. Aoyama, T. Kinoshita and M. Nio, *Theory of the Anomalous Magnetic Moment of the Electron*, *Atoms* **7** (2019) 28 [INSPIRE].

JHEP12(2024)203

[38] A. Czarnecki, W.J. Marciano and A. Vainshtein, *Refinements in electroweak contributions to the muon anomalous magnetic moment*, *Phys. Rev. D* **67** (2003) 073006 [*Erratum ibid.* **73** (2006) 119901] [hep-ph/0212229] [INSPIRE].

[39] C. Gnendiger, D. Stöckinger and H. Stöckinger-Kim, *The electroweak contributions to* $(g-2)_\mu$ *after the Higgs boson mass measurement*, *Phys. Rev. D* **88** (2013) 053005 [arXiv:1306.5546] [INSPIRE].

[40] G. Colangelo et al., *Prospects for precise predictions of* a_μ *in the Standard Model*, arXiv:2203.15810 [INSPIRE].

[41] C. Lehner and A.S. Meyer, *Consistency of hadronic vacuum polarization between lattice QCD and the R-ratio*, *Phys. Rev. D* **101** (2020) 074515 [arXiv:2003.04177] [INSPIRE].

[42] M. Hoferichter and P. Stoffer, *Asymptotic behavior of meson transition form factors*, *JHEP* **05** (2020) 159 [arXiv:2004.06127] [INSPIRE].

[43] M. Knecht, *On some short-distance properties of the fourth-rank hadronic vacuum polarization tensor and the anomalous magnetic moment of the muon*, *JHEP* **08** (2020) 056 [arXiv:2005.09929] [INSPIRE].

[44] P. Masjuan, P. Roig and P. Sánchez-Puertas, *The interplay of transverse degrees of freedom and axial-vector mesons with short-distance constraints in* $g-2$, *J. Phys. G* **49** (2022) 015002 [arXiv:2005.11761] [INSPIRE].

[45] J. Lüdtke and M. Procura, *Effects of longitudinal short-distance constraints on the hadronic light-by-light contribution to the muon* $g-2$, *Eur. Phys. J. C* **80** (2020) 1108 [arXiv:2006.00007] [INSPIRE].

[46] E.-H. Chao et al., *Hadronic light-by-light contribution to* $(g-2)_\mu$ *from lattice QCD with* $SU(3)$ *flavor symmetry*, *Eur. Phys. J. C* **80** (2020) 869 [arXiv:2006.16224] [INSPIRE].

[47] J.A. Miranda and P. Roig, *New* τ*-based evaluation of the hadronic contribution to the vacuum polarization piece of the muon anomalous magnetic moment*, *Phys. Rev. D* **102** (2020) 114017 [arXiv:2007.11019] [INSPIRE].

[48] B.-L. Hoid, M. Hoferichter and B. Kubis, *Hadronic vacuum polarization and vector-meson resonance parameters from* $e^+e^- \to \pi^0\gamma$, *Eur. Phys. J. C* **80** (2020) 988 [arXiv:2007.12696] [INSPIRE].

[49] J. Bijnens, N. Hermansson-Truedsson, L. Laub and A. Rodríguez-Sánchez, *Short-distance HLbL contributions to the muon anomalous magnetic moment beyond perturbation theory*, *JHEP* **10** (2020) 203 [arXiv:2008.13487] [INSPIRE].

[50] G. Colangelo, M. Hoferichter and P. Stoffer, *Constraints on the two-pion contribution to hadronic vacuum polarization*, *Phys. Lett. B* **814** (2021) 136073 [arXiv:2010.07943] [INSPIRE].

[51] J. Bijnens, N. Hermansson-Truedsson, L. Laub and A. Rodríguez-Sánchez, *The two-loop perturbative correction to the* $(g-2)_\mu$ *HLbL at short distances*, *JHEP* **04** (2021) 240 [arXiv:2101.09169] [INSPIRE].

[52] E.-H. Chao et al., *Hadronic light-by-light contribution to* $(g-2)_\mu$ *from lattice QCD: a complete calculation*, *Eur. Phys. J. C* **81** (2021) 651 [arXiv:2104.02632] [INSPIRE].

[53] I. Danilkin, M. Hoferichter and P. Stoffer, *A dispersive estimate of scalar contributions to hadronic light-by-light scattering*, *Phys. Lett. B* **820** (2021) 136502 [arXiv:2105.01666] [INSPIRE].

JHEP12(2024)203

[54] G. Colangelo et al., *Short-distance constraints for the longitudinal component of the hadronic light-by-light amplitude: an update*, *Eur. Phys. J. C* **81** (2021) 702 [arXiv:2106.13222] [INSPIRE].

[55] J. Leutgeb and A. Rebhan, *Hadronic light-by-light contribution to the muon g-2 from holographic QCD with massive pions*, *Phys. Rev. D* **104** (2021) 094017 [arXiv:2108.12345] [INSPIRE].

[56] G. Colangelo et al., *Chiral extrapolation of hadronic vacuum polarization*, *Phys. Lett. B* **825** (2022) 136852 [arXiv:2110.05493] [INSPIRE].

[57] L. Cappiello, O. Catà and G. D'Ambrosio, *Scalar resonances in the hadronic light-by-light contribution to the muon (g-2)*, *Phys. Rev. D* **105** (2022) 056020 [arXiv:2110.05962] [INSPIRE].

[58] A. Miranda, P. Roig and P. Sánchez-Puertas, *Axial-vector exchange contribution to the hyperfine splitting*, *Phys. Rev. D* **105** (2022) 016017 [arXiv:2110.11366] [INSPIRE].

[59] D. Giusti and S. Simula, *Window contributions to the muon hadronic vacuum polarization with twisted-mass fermions*, *PoS* **LATTICE2021** (2022) 189 [arXiv:2111.15329] [INSPIRE].

[60] M. Hoferichter and T. Teubner, *Mixed Leptonic and Hadronic Corrections to the Anomalous Magnetic Moment of the Muon*, *Phys. Rev. Lett.* **128** (2022) 112002 [arXiv:2112.06929] [INSPIRE].

[61] Á. Miramontes, A. Bashir, K. Raya and P. Roig, *Pion and Kaon box contribution to a_μHLbL*, *Phys. Rev. D* **105** (2022) 074013 [arXiv:2112.13916] [INSPIRE].

[62] D. Stamen et al., *Kaon electromagnetic form factors in dispersion theory*, *Eur. Phys. J. C* **82** (2022) 432 [arXiv:2202.11106] [INSPIRE].

[63] D. Boito, M. Golterman, K. Maltman and S. Peris, *Evaluation of the three-flavor quark-disconnected contribution to the muon anomalous magnetic moment from experimental data*, *Phys. Rev. D* **105** (2022) 093003 [arXiv:2203.05070] [INSPIRE].

[64] CHIQCD collaboration, *Muon g-2 with overlap valence fermions*, *Phys. Rev. D* **107** (2023) 034513 [arXiv:2204.01280] [INSPIRE].

[65] C. Aubin, T. Blum, M. Golterman and S. Peris, *Muon anomalous magnetic moment with staggered fermions: Is the lattice spacing small enough?*, *Phys. Rev. D* **106** (2022) 054503 [arXiv:2204.12256] [INSPIRE].

[66] G. Colangelo et al., *Data-driven evaluations of Euclidean windows to scrutinize hadronic vacuum polarization*, *Phys. Lett. B* **833** (2022) 137313 [arXiv:2205.12963] [INSPIRE].

[67] M. Cè et al., *Window observable for the hadronic vacuum polarization contribution to the muon g-2 from lattice QCD*, *Phys. Rev. D* **106** (2022) 114502 [arXiv:2206.06582] [INSPIRE].

[68] EXTENDED TWISTED MASS collaboration, *Lattice calculation of the short and intermediate time-distance hadronic vacuum polarization contributions to the muon magnetic moment using twisted-mass fermions*, *Phys. Rev. D* **107** (2023) 074506 [arXiv:2206.15084] [INSPIRE].

[69] G. Colangelo, M. Hoferichter, B. Kubis and P. Stoffer, *Isospin-breaking effects in the two-pion contribution to hadronic vacuum polarization*, *JHEP* **10** (2022) 032 [arXiv:2208.08993] [INSPIRE].

[70] V. Biloshytskyi et al., *Forward light-by-light scattering and electromagnetic correction to hadronic vacuum polarization*, *JHEP* **03** (2023) 194 [arXiv:2209.02149] [INSPIRE].

JHEP12(2024)203

[71] D. Boito, M. Golterman, K. Maltman and S. Peris, *Data-based determination of the isospin-limit light-quark-connected contribution to the anomalous magnetic moment of the muon*, *Phys. Rev. D* **107** (2023) 074001 [arXiv:2211.11055] [INSPIRE].

[72] J. Leutgeb, J. Mager and A. Rebhan, *Hadronic light-by-light contribution to the muon g-2 from holographic QCD with solved $U(1)A$ problem*, *Phys. Rev. D* **107** (2023) 054021 [arXiv:2211.16562] [INSPIRE].

[73] J. Bijnens, N. Hermansson-Truedsson and A. Rodríguez-Sánchez, *Constraints on the hadronic light-by-light in the Melnikov-Vainshtein regime*, *JHEP* **02** (2023) 167 [arXiv:2211.17183] [INSPIRE].

[74] P. Colangelo, F. Giannuzzi and S. Nicotri, *π^0,η,η' two-photon transition form factors in the holographic soft-wall model and contributions to $(g-2)\mu$*, *Phys. Lett. B* **840** (2023) 137878 [arXiv:2301.06456] [INSPIRE].

[75] Fermilab Lattice et al. collaborations, *Light-quark connected intermediate-window contributions to the muon g-2 hadronic vacuum polarization from lattice QCD*, *Phys. Rev. D* **107** (2023) 114514 [arXiv:2301.08274] [INSPIRE].

[76] RBC and UKQCD collaborations, *Update of Euclidean windows of the hadronic vacuum polarization*, *Phys. Rev. D* **108** (2023) 054507 [arXiv:2301.08696] [INSPIRE].

[77] M. Davier et al., *The euclidean Adler function and its interplay with $\Delta\alpha^{had}_{QED}$ and α_s*, *JHEP* **04** (2023) 067 [arXiv:2302.01359] [INSPIRE].

[78] S.-J. Wang, Z. Fang and L.-Y. Dai, *Two body final states production in electron-positron annihilation and their contributions to $(g-2)_\mu$*, *JHEP* **07** (2023) 037 [arXiv:2302.08859] [INSPIRE].

[79] J. Lüdtke, M. Procura and P. Stoffer, *Dispersion relations for hadronic light-by-light scattering in triangle kinematics*, *JHEP* **04** (2023) 125 [arXiv:2302.12264] [INSPIRE].

[80] R. Escribano, J.A. Miranda and P. Roig, *Radiative corrections to the $\tau^- \to (P1P2)^- v\tau(P1,2=\pi,K)$ decays*, *Phys. Rev. D* **109** (2024) 053003 [arXiv:2303.01362] [INSPIRE].

[81] T. Blum et al., *Hadronic light-by-light contribution to the muon anomaly from lattice QCD with infinite volume QED at physical pion mass*, arXiv:2304.04423 [INSPIRE].

[82] P. Masjuan, A. Miranda and P. Roig, *τ data-driven evaluation of Euclidean windows for the hadronic vacuum polarization*, *Phys. Lett. B* **850** (2024) 138492 [arXiv:2305.20005] [INSPIRE].

[83] A.V. Nesterenko, *Effects of the quark flavour thresholds in the hadronic vacuum polarization contributions to the muon anomalous magnetic moment*, *J. Phys. G* **51** (2024) 015005 [arXiv:2306.16392] [INSPIRE].

[84] G. Benton et al., *Data-Driven Determination of the Light-Quark Connected Component of the Intermediate-Window Contribution to the Muon $g-2$*, *Phys. Rev. Lett.* **131** (2023) 251803 [arXiv:2306.16808] [INSPIRE].

[85] M. Hoferichter et al., *Phenomenological Estimate of Isospin Breaking in Hadronic Vacuum Polarization*, *Phys. Rev. Lett.* **131** (2023) 161905 [arXiv:2307.02532] [INSPIRE].

[86] M. Davier et al., *Hadronic vacuum polarization: Comparing lattice QCD and data-driven results in systematically improvable ways*, *Phys. Rev. D* **109** (2024) 076019 [arXiv:2308.04221] [INSPIRE].

JHEP12(2024)203

[87] M. Davier et al., *Tensions in $e^+e^- \to \pi^+\pi^-(\gamma)$ measurements: the new landscape of data-driven hadronic vacuum polarization predictions for the muon $g-2$*, *Eur. Phys. J. C* **84** (2024) 721 [arXiv:2312.02053] [INSPIRE].

[88] P. Colangelo, F. Giannuzzi and S. Nicotri, *Hadronic light-by-light scattering contributions to (g-2)μ from axial-vector and tensor mesons in the holographic soft-wall model*, *Phys. Rev. D* **109** (2024) 094036 [arXiv:2402.07579] [INSPIRE].

[89] M. Hoferichter, P. Stoffer and M. Zillinger, *An optimized basis for hadronic light-by-light scattering*, *JHEP* **04** (2024) 092 [arXiv:2402.14060] [INSPIRE].

[90] D. Boito, C.Y. London, P. Masjuan and C. Rojas, *Model-independent extrapolation of MUonE data with Padé and D-Log approximants*, *Phys. Rev. D* **110** (2024) 074012 [arXiv:2405.13638] [INSPIRE].

[91] A. Boccaletti et al., *High precision calculation of the hadronic vacuum polarisation contribution to the muon anomaly*, arXiv:2407.10913 [INSPIRE].

[92] L. Di Luzio, A. Keshavarzi, A. Masiero and P. Paradisi, *Model Independent Tests of the Hadronic Vacuum Polarization Contribution to the Muon $g-2$*, arXiv:2408.01123 [INSPIRE].

[93] S. Lahert et al., *The two-pion contribution to the hadronic vacuum polarization with staggered quarks*, arXiv:2409.00756 [INSPIRE].

[94] A. Keshavarzi, D. Nomura, T. Teubner and A. Wright, *Muon $g-2$: blinding for data-driven hadronic vacuum polarization*, arXiv:2409.02827 [INSPIRE].

[95] E. Budassi et al., *Pion pair production in e^+e^- annihilation at next-to-leading order matched to Parton Shower*, arXiv:2409.03469 [INSPIRE].

[96] CMD-3 collaboration, *Measurement of the $e^+e^- \to \pi+\pi-$ cross section from threshold to 1.2 GeV with the CMD-3 detector*, *Phys. Rev. D* **109** (2024) 112002 [arXiv:2302.08834] [INSPIRE].

[97] CMD-3 collaboration, *Measurement of the Pion Form Factor with CMD-3 Detector and its Implication to the Hadronic Contribution to Muon $(g-2)$*, *Phys. Rev. Lett.* **132** (2024) 231903 [arXiv:2309.12910] [INSPIRE].

[98] E. de Rafael, *Hadronic contributions to the muon $g-2$ and low-energy QCD*, *Phys. Lett. B* **322** (1994) 239 [hep-ph/9311316] [INSPIRE].

[99] M. Hayakawa, T. Kinoshita and A.I. Sanda, *Hadronic light by light scattering effect on muon $g-2$*, *Phys. Rev. Lett.* **75** (1995) 790 [hep-ph/9503463] [INSPIRE].

[100] J. Bijnens, E. Pallante and J. Prades, *Hadronic light by light contributions to the muon $g-2$ in the large N_c limit*, *Phys. Rev. Lett.* **75** (1995) 1447 [*Erratum ibid.* **75** (1995) 3781] [hep-ph/9505251] [INSPIRE].

[101] J. Bijnens, E. Pallante and J. Prades, *Analysis of the hadronic light by light contributions to the muon $g-2$*, *Nucl. Phys. B* **474** (1996) 379 [hep-ph/9511388] [INSPIRE].

[102] M. Hayakawa, T. Kinoshita and A.I. Sanda, *Hadronic light by light scattering contribution to muon $g-2$*, *Phys. Rev. D* **54** (1996) 3137 [hep-ph/9601310] [INSPIRE].

[103] M. Hayakawa and T. Kinoshita, *Pseudoscalar pole terms in the hadronic light by light scattering contribution to muon $g-2$*, *Phys. Rev. D* **57** (1998) 465 [*Erratum ibid.* **66** (2002) 019902] [hep-ph/9708227] [INSPIRE].

[104] J. Bijnens, E. Pallante and J. Prades, *Comment on the pion pole part of the light by light contribution to the muon $g-2$*, *Nucl. Phys. B* **626** (2002) 410 [hep-ph/0112255] [INSPIRE].

JHEP12(2024)203

[105] G. 't Hooft, *A Planar Diagram Theory for Strong Interactions*, *Nucl. Phys. B* **72** (1974) 461 [INSPIRE].

[106] G. 't Hooft, *A Two-Dimensional Model for Mesons*, *Nucl. Phys. B* **75** (1974) 461 [INSPIRE].

[107] E. Witten, *Baryons in the 1/n Expansion*, *Nucl. Phys. B* **160** (1979) 57 [INSPIRE].

[108] S. Weinberg, *Phenomenological Lagrangians*, *Physica A* **96** (1979) 327 [INSPIRE].

[109] J. Gasser and H. Leutwyler, *Chiral Perturbation Theory to One Loop*, *Annals Phys.* **158** (1984) 142 [INSPIRE].

[110] J. Gasser and H. Leutwyler, *Chiral Perturbation Theory: Expansions in the Mass of the Strange Quark*, *Nucl. Phys. B* **250** (1985) 465 [INSPIRE].

[111] M. Knecht and A. Nyffeler, *Hadronic light by light corrections to the muon $g-2$: The pion pole contribution*, *Phys. Rev. D* **65** (2002) 073034 [hep-ph/0111058] [INSPIRE].

[112] V. Pauk and M. Vanderhaeghen, *Anomalous magnetic moment of the muon in a dispersive approach*, *Phys. Rev. D* **90** (2014) 113012 [arXiv:1409.0819] [INSPIRE].

[113] J. Leutgeb and A. Rebhan, *Axial vector transition form factors in holographic QCD and their contribution to the anomalous magnetic moment of the muon*, *Phys. Rev. D* **101** (2020) 114015 [arXiv:1912.01596] [INSPIRE].

[114] L. Cappiello et al., *Axial-vector and pseudoscalar mesons in the hadronic light-by-light contribution to the muon $(g-2)$*, *Phys. Rev. D* **102** (2020) 016009 [arXiv:1912.02779] [INSPIRE].

[115] M. Zanke, M. Hoferichter and B. Kubis, *On the transition form factors of the axial-vector resonance $f_1(1285)$ and its decay into e^+e^-*, *JHEP* **07** (2021) 106 [arXiv:2103.09829] [INSPIRE].

[116] J. Leutgeb, J. Mager and A. Rebhan, *Holographic QCD and the muon anomalous magnetic moment*, *Eur. Phys. J. C* **81** (2021) 1008 [arXiv:2110.07458] [INSPIRE].

[117] A.E. Radzhabov, A.S. Zhevlakov, A.P. Martynenko and F.A. Martynenko, *Light-by-light contribution to the muon anomalous magnetic moment from the axial-vector mesons exchanges within the nonlocal quark model*, *Phys. Rev. D* **108** (2023) 014033 [arXiv:2301.12641] [INSPIRE].

[118] M. Hoferichter, B. Kubis and M. Zanke, *Axial-vector transition form factors and $e^+e^- \to f_1\pi^+\pi^-$*, *JHEP* **08** (2023) 209 [arXiv:2307.14413] [INSPIRE].

[119] G. Eichmann, C.S. Fischer, E. Weil and R. Williams, *Single pseudoscalar meson pole and pion box contributions to the anomalous magnetic moment of the muon*, *Phys. Lett. B* **797** (2019) 134855 [*Erratum ibid.* **799** (2019) 135029] [arXiv:1903.10844] [INSPIRE].

[120] K. Raya, A. Bashir and P. Roig, *Contribution of neutral pseudoscalar mesons to a_μ^{HLbL} within a Schwinger-Dyson equations approach to QCD*, *Phys. Rev. D* **101** (2020) 074021 [arXiv:1910.05960] [INSPIRE].

[121] G. Ecker et al., *Chiral Lagrangians for Massive Spin 1 Fields*, *Phys. Lett. B* **223** (1989) 425 [INSPIRE].

[122] K. Kampf and J. Novotný, *Resonance saturation in the odd-intrinsic parity sector of low-energy QCD*, *Phys. Rev. D* **84** (2011) 014036 [arXiv:1104.3137] [INSPIRE].

[123] P. Roig, A. Guevara and G. López Castro, *$VV'P$ form factors in resonance chiral theory and the $\pi-\eta-\eta'$ light-by-light contribution to the muon $g-2$*, *Phys. Rev. D* **89** (2014) 073016 [arXiv:1401.4099] [INSPIRE].

JHEP12(2024)203

[124] A. Guevara, P. Roig and J.J. Sanz-Cillero, *Pseudoscalar pole light-by-light contributions to the muon $(g-2)$ in Resonance Chiral Theory*, *JHEP* **06** (2018) 160 [arXiv:1803.08099] [INSPIRE].

[125] H. Czyz, S. Ivashyn, A. Korchin and O. Shekhovtsova, *Two-photon form factors of the π^0, η and η' mesons in the chiral theory with resonances*, *Phys. Rev. D* **85** (2012) 094010 [arXiv:1202.1171] [INSPIRE].

[126] T. Kadavý, K. Kampf and J. Novotný, *On the three-point order parameters of chiral symmetry breaking*, *JHEP* **03** (2023) 118 [arXiv:2206.02579] [INSPIRE].

[127] P.D. Ruiz-Femenía, A. Pich and J. Portolés, *Odd intrinsic parity processes within the resonance effective theory of QCD*, *JHEP* **07** (2003) 003 [hep-ph/0306157] [INSPIRE].

[128] V. Cirigliano et al., *Towards a consistent estimate of the chiral low-energy constants*, *Nucl. Phys. B* **753** (2006) 139 [hep-ph/0603205] [INSPIRE].

[129] V. Cirigliano, G. Ecker, H. Neufeld and A. Pich, *Meson resonances, large N_c and chiral symmetry*, *JHEP* **06** (2003) 012 [hep-ph/0305311] [INSPIRE].

[130] Z.-H. Guo and J.J. Sanz-Cillero, *$\pi\pi$-scattering lengths at $O(p^6)$ revisited*, *Phys. Rev. D* **79** (2009) 096006 [arXiv:0903.0782] [INSPIRE].

[131] V. Mateu and J. Portolés, *Form-factors in radiative pion decay*, *Eur. Phys. J. C* **52** (2007) 325 [arXiv:0706.1039] [INSPIRE].

[132] T. Kadavý, K. Kampf and J. Novotný, *OPE of Green functions of chiral currents*, *JHEP* **10** (2020) 142 [arXiv:2006.13006] [INSPIRE].

[133] J. Wess and B. Zumino, *Consequences of anomalous Ward identities*, *Phys. Lett. B* **37** (1971) 95 [INSPIRE].

[134] E. Witten, *Global Aspects of Current Algebra*, *Nucl. Phys. B* **223** (1983) 422 [INSPIRE].

[135] S.L. Adler, *Axial vector vertex in spinor electrodynamics*, *Phys. Rev.* **177** (1969) 2426 [INSPIRE].

[136] J.S. Bell and R. Jackiw, *A PCAC puzzle: $\pi^0 \to \gamma\gamma$ in the σ model*, *Nuovo Cim. A* **60** (1969) 47 [INSPIRE].

[137] J. Bijnens, L. Girlanda and P. Talavera, *The Anomalous chiral Lagrangian of order p^6*, *Eur. Phys. J. C* **23** (2002) 539 [hep-ph/0110400] [INSPIRE].

[138] P. Roig and J.J. Sanz Cillero, *Consistent high-energy constraints in the anomalous QCD sector*, *Phys. Lett. B* **733** (2014) 158 [arXiv:1312.6206] [INSPIRE].

[139] J. Bijnens, G. Colangelo and G. Ecker, *The Mesonic chiral Lagrangian of order p^6*, *JHEP* **02** (1999) 020 [hep-ph/9902437] [INSPIRE].

[140] V. Bernard, N. Kaiser and U.G. Meissner, *Chiral perturbation theory in the presence of resonances: Application to $\pi\pi$ and pi K scattering*, *Nucl. Phys. B* **364** (1991) 283 [INSPIRE].

[141] J.J. Sanz-Cillero, *Pion and kaon decay constants: Lattice versus resonance chiral theory*, *Phys. Rev. D* **70** (2004) 094033 [hep-ph/0408080] [INSPIRE].

[142] Z.-H. Guo and J.J. Sanz-Cillero, *Resonance effects in pion and kaon decay constants*, *Phys. Rev. D* **89** (2014) 094024 [arXiv:1403.0855] [INSPIRE].

[143] Particle Data Group collaboration, *Review of Particle Physics*, *PTEP* **2022** (2022) 083C01 [INSPIRE].

[144] J. Schechter, A. Subbaraman and H. Weigel, *Effective hadron dynamics: From meson masses to the proton spin puzzle*, *Phys. Rev. D* **48** (1993) 339 [hep-ph/9211239] [INSPIRE].

JHEP12(2024)203

[145] A. Bramon, R. Escribano and M.D. Scadron, *The η-η' mixing angle revisited*, *Eur. Phys. J. C* **7** (1999) 271 [hep-ph/9711229] [INSPIRE].

[146] T. Feldmann, *Quark structure of pseudoscalar mesons*, *Int. J. Mod. Phys. A* **15** (2000) 159 [hep-ph/9907491] [INSPIRE].

[147] R. Escribano and J.-M. Frère, *Study of the η-eta$'$ system in the two mixing angle scheme*, *JHEP* **06** (2005) 029 [hep-ph/0501072] [INSPIRE].

[148] V.A. Nesterenko and A.V. Radyushkin, *Local Quark-Hadron Duality and Nucleon Form-factors in QCD*, *Phys. Lett. B* **128** (1983) 439 [INSPIRE].

[149] V.A. Novikov et al., *Use and Misuse of QCD Sum Rules, Factorization and Related Topics*, *Nucl. Phys. B* **237** (1984) 525 [INSPIRE].

[150] S.J. Brodsky and G.R. Farrar, *Scaling Laws at Large Transverse Momentum*, *Phys. Rev. Lett.* **31** (1973) 1153 [INSPIRE].

[151] G.P. Lepage and S.J. Brodsky, *Exclusive Processes in Perturbative Quantum Chromodynamics*, *Phys. Rev. D* **22** (1980) 2157 [INSPIRE].

[152] H. Leutwyler, *On the 1/N expansion in chiral perturbation theory*, *Nucl. Phys. B Proc. Suppl.* **64** (1998) 223 [hep-ph/9709408] [INSPIRE].

[153] Z.-H. Guo and P. Roig, *One meson radiative tau decays*, *Phys. Rev. D* **82** (2010) 113016 [arXiv:1009.2542] [INSPIRE].

[154] M.A. Arroyo-Ureña et al., *Radiative corrections to $\tau \to \pi(K)\nu\tau[\gamma]$: A reliable new physics test*, *Phys. Rev. D* **104** (2021) L091502 [arXiv:2107.04603] [INSPIRE].

[155] M.A. Arroyo-Ureña et al., *One-loop determination of $\tau \to \pi(K)\nu_\tau[\gamma]$ branching ratios and new physics tests*, *JHEP* **02** (2022) 173 [arXiv:2112.01859] [INSPIRE].

[156] Z.-H. Guo, *Study of tau- $\to$ V P- nu(tau) in the framework of resonance chiral theory*, *Phys. Rev. D* **78** (2008) 033004 [arXiv:0806.4322] [INSPIRE].

[157] D.G. Dumm, P. Roig, A. Pich and J. Portolés, *Hadron structure in tau $\to$ KK pi nu (tau) decays*, *Phys. Rev. D* **81** (2010) 034031 [arXiv:0911.2640] [INSPIRE].

[158] D. Gómez Dumm and P. Roig, *Resonance Chiral Lagrangian analysis of $\tau^- \to \eta^{(\prime)}\pi^-\pi^0\nu_\tau$ decays*, *Phys. Rev. D* **86** (2012) 076009 [arXiv:1208.1212] [INSPIRE].

[159] D.G. Dumm, P. Roig, A. Pich and J. Portolés, *$\tau \to \pi\pi\pi\nu_\tau$ decays and the a(1)(1260) off-shell width revisited*, *Phys. Lett. B* **685** (2010) 158 [arXiv:0911.4436] [INSPIRE].

[160] O. Shekhovtsova, T. Przedzinski, P. Roig and Z. Was, *Resonance chiral Lagrangian currents and τ decay Monte Carlo*, *Phys. Rev. D* **86** (2012) 113008 [arXiv:1203.3955] [INSPIRE].

[161] I.M. Nugent et al., *Resonance chiral Lagrangian currents and experimental data for $\tau^- \to \pi^-\pi^-\pi^+\nu_\tau$*, *Phys. Rev. D* **88** (2013) 093012 [arXiv:1310.1053] [INSPIRE].

[162] K. Kampf, J. Novotný and P. Sánchez-Puertas, *Radiative corrections to double-Dalitz decays revisited*, *Phys. Rev. D* **97** (2018) 056010 [arXiv:1801.06067] [INSPIRE].

[163] BaBar collaboration, *Measurement of the gamma gamma* $\to$ pi0 transition form factor*, *Phys. Rev. D* **80** (2009) 052002 [arXiv:0905.4778] [INSPIRE].

[164] BaBar collaboration, *Measurement of the $\gamma\gamma^* \to \eta$ and $\gamma\gamma* \to \eta'$ transition form factors*, *Phys. Rev. D* **84** (2011) 052001 [arXiv:1101.1142] [INSPIRE].

[165] Belle collaboration, *Measurement of $\gamma\gamma^* \to \pi^0$ transition form factor at Belle*, *Phys. Rev. D* **86** (2012) 092007 [arXiv:1205.3249] [INSPIRE].

JHEP12(2024)203

[166] CELLO collaboration, *A measurement of the pi0, eta and eta-prime electromagnetic form-factors*, *Z. Phys. C* **49** (1991) 401 [INSPIRE].

[167] CLEO collaboration, *Measurements of the meson-photon transition form-factors of light pseudoscalar mesons at large momentum transfer*, *Phys. Rev. D* **57** (1998) 33 [hep-ex/9707031] [INSPIRE].

[168] L3 collaboration, *Measurement of eta-prime (958) formation in two photon collisions at LEP-1*, *Phys. Lett. B* **418** (1998) 399 [INSPIRE].

[169] BABAR collaboration, *Measurement of the $\gamma^\star\gamma^\star \to \eta'$ transition form factor*, *Phys. Rev. D* **98** (2018) 112002 [arXiv:1808.08038] [INSPIRE].

[170] A. Gérardin et al., *Lattice calculation of the π^0, η and η' transition form factors and the hadronic light-by-light contribution to the muon $g-2$*, arXiv:2305.04570 [INSPIRE].

[171] EXTENDED TWISTED MASS collaboration, *$\eta \to \gamma^*\gamma^*$ transition form factor and the hadronic light-by-light η-pole contribution to the muon $g-2$ from lattice QCD*, *Phys. Rev. D* **108** (2023) 054509 [arXiv:2212.06704] [INSPIRE].

[172] EXTENDED TWISTED MASS collaboration, *Pion transition form factor from twisted-mass lattice QCD and the hadronic light-by-light π^0-pole contribution to the muon $g-2$*, *Phys. Rev. D* **108** (2023) 094514 [arXiv:2308.12458] [INSPIRE].

[173] T. Feldmann, P. Kroll and B. Stech, *Mixing and decay constants of pseudoscalar mesons*, *Phys. Rev. D* **58** (1998) 114006 [hep-ph/9802409] [INSPIRE].

[174] R. Kaiser and H. Leutwyler, *Large N_c in chiral perturbation theory*, *Eur. Phys. J. C* **17** (2000) 623 [hep-ph/0007101] [INSPIRE].

[175] S.V. Mikhailov and N.G. Stefanis, *Transition form factors of the pion in light-cone QCD sum rules with next-to-next-to-leading order contributions*, *Nucl. Phys. B* **821** (2009) 291 [arXiv:0905.4004] [INSPIRE].

[176] H.L.L. Roberts et al., *Abelian anomaly and neutral pion production*, *Phys. Rev. C* **82** (2010) 065202 [arXiv:1009.0067] [INSPIRE].

[177] S.S. Agaev, V.M. Braun, N. Offen and F.A. Porkert, *Light Cone Sum Rules for the $\pi^0\gamma^*\gamma$ Form Factor Revisited*, *Phys. Rev. D* **83** (2011) 054020 [arXiv:1012.4671] [INSPIRE].

[178] S.J. Brodsky, F.-G. Cao and G.F. de Teramond, *Evolved QCD predictions for the meson-photon transition form factors*, *Phys. Rev. D* **84** (2011) 033001 [arXiv:1104.3364] [INSPIRE].

[179] A.P. Bakulev, S.V. Mikhailov, A.V. Pimikov and N.G. Stefanis, *Pion-photon transition: The New QCD frontier*, *Phys. Rev. D* **84** (2011) 034014 [arXiv:1105.2753] [INSPIRE].

[180] S.J. Brodsky, F.-G. Cao and G.F. de Teramond, *Meson Transition Form Factors in Light-Front Holographic QCD*, *Phys. Rev. D* **84** (2011) 075012 [arXiv:1105.3999] [INSPIRE].

[181] N.G. Stefanis, A.P. Bakulev, S.V. Mikhailov and A.V. Pimikov, *Can We Understand an Auxetic Pion-Photon Transition Form Factor within QCD?*, *Phys. Rev. D* **87** (2013) 094025 [arXiv:1202.1781] [INSPIRE].

[182] A.P. Bakulev, S.V. Mikhailov, A.V. Pimikov and N.G. Stefanis, *Comparing antithetic trends of data for the pion-photon transition form factor*, *Phys. Rev. D* **86** (2012) 031501 [arXiv:1205.3770] [INSPIRE].

[183] S.S. Agaev, V.M. Braun, N. Offen and F.A. Porkert, *BELLE Data on the $\pi^0\gamma * \gamma$ Form Factor: A Game Changer?*, *Phys. Rev. D* **86** (2012) 077504 [arXiv:1206.3968] [INSPIRE].

JHEP12(2024)203

[184] S.S. Agaev et al., *Transition form factors $\gamma^*\gamma \to \eta$ and $\gamma^*\gamma \to \eta'$ in QCD*, *Phys. Rev. D* **90** (2014) 074019 [arXiv:1409.4311] [INSPIRE].

[185] K. Raya et al., *Structure of the neutral pion and its electromagnetic transition form factor*, *Phys. Rev. D* **93** (2016) 074017 [arXiv:1510.02799] [INSPIRE].

[186] G. Eichmann, C.S. Fischer, E. Weil and R. Williams, *On the large-Q^2 behavior of the pion transition form factor*, *Phys. Lett. B* **774** (2017) 425 [arXiv:1704.05774] [INSPIRE].

[187] N.G. Stefanis, *Pion-photon transition form factor in light cone sum rules and tests of asymptotics*, *Phys. Rev. D* **102** (2020) 034022 [arXiv:2006.10576] [INSPIRE].

[188] S.J. Brodsky and G.P. Lepage, *Large Angle Two Photon Exclusive Channels in Quantum Chromodynamics*, *Phys. Rev. D* **24** (1981) 1808 [INSPIRE].

[189] Y.-H. Chen, Z.-H. Guo and H.-Q. Zheng, *Study of η-η' mixing from radiative decay processes*, *Phys. Rev. D* **85** (2012) 054018 [arXiv:1201.2135] [INSPIRE].

[190] L.Y. Dai, J. Portolés and O. Shekhovtsova, *Three pseudoscalar meson production in e^+e^- annihilation*, *Phys. Rev. D* **88** (2013) 056001 [arXiv:1305.5751] [INSPIRE].

[191] Y.-H. Chen, Z.-H. Guo and H.-Q. Zheng, *Radiative transition processes of light vector resonances in a chiral framework*, *Phys. Rev. D* **90** (2014) 034013 [arXiv:1311.3366] [INSPIRE].

[192] Y.-H. Chen, Z.-H. Guo and B.-S. Zou, *Unified study of $J/\psi \to PV$, $P\gamma^{(*)}$ and light hadron radiative processes*, *Phys. Rev. D* **91** (2015) 014010 [arXiv:1411.1159] [INSPIRE].

[193] PrimEx collaboration, *A new Measurement of the π^0 Radiative Decay Width*, *Phys. Rev. Lett.* **106** (2011) 162303 [arXiv:1009.1681] [INSPIRE].

[194] PrimEx-II collaboration, *Precision measurement of the neutral pion lifetime*, *Science* **368** (2020) 506 [INSPIRE].

[195] KLOE-2 collaboration, *Measurement of η meson production in $\gamma\gamma$ interactions and $\Gamma(\eta \to \gamma\gamma)$ with the KLOE detector*, *JHEP* **01** (2013) 119 [arXiv:1211.1845] [INSPIRE].

[196] S. Holz, M. Hoferichter, B.-L. Hoid and B. Kubis, *A precision evaluation of the η- and η'-pole contributions to hadronic light-by-light scattering in the anomalous magnetic moment of the muon*, arXiv:2411.08098 [INSPIRE].

[197] R. Escribano and S. Gonzàlez-Solís, *A data-driven approach to π^0, η and η' single and double Dalitz decays*, *Chin. Phys. C* **42** (2018) 023109 [arXiv:1511.04916] [INSPIRE].

[198] J.S.R. Chisholm, *Rational approximants defined from double power series*, *Math. Comput.* **27** (1973) 841.

[199] J.S.R. Chisholm and J. McEwan, *Rational approximants defined from power series in N variables*, *Proc. Roy. Soc. Lond. A* **336** (1974) 421.

[200] R.H. Jones, *General rational approximants in N-variables*, *J. Approx. Theor.* **16** (1976) 201.

[201] P. Masjuan and P. Sánchez-Puertas, *Phenomenology of bivariate approximants: the $\pi^0 \to e^+e^-$ case and its impact on the electron and muon $g-2$*, arXiv:1504.07001 [INSPIRE].

[202] P. Masjuan and P. Sánchez-Puertas, *η and η' decays into lepton pairs*, *JHEP* **08** (2016) 108 [arXiv:1512.09292] [INSPIRE].

[203] R. Escribano, S. Gonzàlez-Solís, P. Masjuan and P. Sánchez-Puertas, *η' transition form factor from space- and timelike experimental data*, *Phys. Rev. D* **94** (2016) 054033 [arXiv:1512.07520] [INSPIRE].

JHEP12(2024)203

[204] A. Nyffeler, *Precision of a data-driven estimate of hadronic light-by-light scattering in the muon $g-2$: Pseudoscalar-pole contribution*, *Phys. Rev. D* **94** (2016) 053006 [arXiv:1602.03398] [INSPIRE].

[205] RBC/UKQCD collaboration, X. Feng, *Update from RBC/UKQCD* talk at the *Seventh plenary workshop of the muon $g-2$ theory initiative workshop, light meson decays at hlbl-update from rbc-ukqcd*, KEK, Tsukuba, Japan, September 12 (2024) [https://conference-indico.kek.jp/event/257/contributions/5797].

[206] G.P. Lepage, *Adaptive multidimensional integration: VEGAS enhanced*, *J. Comput. Phys.* **439** (2021) 110386 [arXiv:2009.05112] [INSPIRE].

[207] G.P. Lepage, *A New Algorithm for Adaptive Multidimensional Integration*, *J. Comput. Phys.* **27** (1978) 192 [INSPIRE].

[208] M. Hoferichter et al., *Pion-pole contribution to hadronic light-by-light scattering in the anomalous magnetic moment of the muon*, *Phys. Rev. Lett.* **121** (2018) 112002 [arXiv:1805.01471] [INSPIRE].

[209] X.-K. Guo, Z.-H. Guo, J.A. Oller and J.J. Sanz-Cillero, *Scrutinizing the η-η' mixing, masses and pseudoscalar decay constants in the framework of $U(3)$ chiral effective field theory*, *JHEP* **06** (2015) 175 [arXiv:1503.02248] [INSPIRE].

[210] F. Guerrero and A. Pich, *Effective field theory description of the pion form-factor*, *Phys. Lett. B* **412** (1997) 382 [hep-ph/9707347] [INSPIRE].

[211] G.P. Lepage and S.J. Brodsky, *Exclusive Processes in Quantum Chromodynamics: Evolution Equations for Hadronic Wave Functions and the Form-Factors of Mesons*, *Phys. Lett. B* **87** (1979) 359 [INSPIRE].

[212] V.M. Braun, G.P. Korchemsky and D. Müller, *The uses of conformal symmetry in QCD*, *Prog. Part. Nucl. Phys.* **51** (2003) 311 [hep-ph/0306057] [INSPIRE].

JHEP12(2024)203